SHAPE OPTIMIZATION OF WHEELED EXCAVATOR LOWER
CHASSIS

A THESIS SUBMITTED TO
THE GRADUATE SCHOOL OF NATURAL AND APPLIED SCIENCES
OF
MIDDLE EAST TECHNICAL UNIVERSITY

BY

ERKAL ÖZBAYRAMOĞLU

IN PARTIAL FULFILLMENT OF THE REQUIREMENTS
FOR
THE DEGREE OF MASTER OF SCIENCE
IN
MECHANICAL ENGINEERING

AUGUST 2008

Approval of the thesis:

SHAPE OPTIMIZATION OF WHEELED EXCAVATOR LOWER CHASSIS

submitted by **ERKAL ÖZBAYRAMOĞLU** in partial fulfillment of the requirements for the degree of **Master of Science in Mechanical Engineering Department, Middle East Technical University** by,

Prof. Dr. Canan Özgen
Dean, Graduate School of **Natural and Applied Sciences**   _____

Prof. Dr. Kemal İder
Head of Department, **Mechanical Engineering**   _____

Prof. Dr. Eres Söylemez
Supervisor, **Mechanical Engineering Dept., METU**   _____

Examining Committee Members:

Prof. Dr. Mehmet Çalışkan (*)
Mechanical Engineering Dept., METU   _____

Prof. Dr. Eres Söylemez (**)
Mechanical Engineering Dept., METU   _____

Prof. Dr. Haluk Darendeliler
Mechanical Engineering Dept., METU   _____

Prof. Dr. Suat Kadıoğlu
Mechanical Engineering Dept., METU   _____

Assoc. Prof. Dr. Bora Yıldırım
Mechanical Engineering Dept., Hacettepe University   _____

                                          Date: _____

(*)   Head of Examining Committee
(**)   Supervisor

I hereby declare that all information in this document has been obtained and presented in accordance with academic rules and ethical conduct. I also declare that, as required by these rules and conduct, I have fully cited and referenced all material and results that are not original to this work.

Name, Last name : Erkal Özbayramoğlu

Signature   :

ABSTRACT

SHAPE OPTIMIZATION OF WHEELED EXCAVATOR LOWER CHASSIS

Özbayramoğlu, Erkal

M.S., Department of Mechanical Engineering

Supervisor: Prof. Dr. Eres Söylemez

August 2008, 81 pages

The aim of this study is to perform the shape optimization of the lower chassis of the wheeled excavator. A computer program is designed to generate parametric Finite Element Analysis (FEA) of the structure by using the commercial program, MSC. Marc-Mentat. The model parameters are generated in the Microsoft Excel platform and the analysis data is collected by the Python based computer codes. The previously developed software Smart Designer [5], which performs the shape optimization of an excavator boom by using genetic algorithm, is modified and embedded in the designed program.

Keywords: Finite Element Analysis, Shape Optimization, Chassis, Wheeled Excavator, Genetic Algorithm

ÖZ

LASTİK TEKERLEKLİ EKSKAVATÖRÜN ALT ŞASİSİNİN ŞEKİL OPTİMİZASYONU

Özbayramoğlu, Erkal

Yüksek Lisans, Makina Mühendisliği Bölümü

Tez Yöneticisi: Prof. Dr. Eres Söylemez

Ağustos 2008, 81 sayfa

Bu çalışmada, lastik tekerlekli ekskavatörün alt şasisinin şekil optimizasyonunun yapılması amaçlanmıştır. MSC. Marc-Mentat ticari programı kullanılarak yapının parametrik olarak sonlu elemanlar analizini oluşturmak için bilgisayar programı tasarlanmıştır. Model parametreleri Microsoft Excel ortamında oluşturulmuştur. Analiz sonuç verileri Python tabanlı kodlar tarafından alınmaktadır. Önceden geliştirilmiş olan ekskavatör bomunu genetik algoritma kullanarak şekil optimizasyonu yapan Smart Designer [5] programı modifiye edilmiş ve tasarlanan programla uygun çalışır hale getirilmiştir.

Anahtar kelimeler: Sonlu Elemanlar Analizi, Şekil Optimizasyonu, Şasi, Lastik Tekerlekli Ekskavatör, Genetik Algoritma

To My Family and My Love Esen

ACKNOWLEDGMENTS

TABLE OF CONTENTS

LIST OF FIGURES

FIGURES

LIST OF SYMBOLS AND ABBREVIATIONS

SYMBOLS

F_{arm} : Arm Breakout Force

s_1 : Length of Boom Cylinder

s_2 : Length of Arm Cylinder

s_3 : Length of Bucket Cylinder

θ_{uc} : Angle between the Upper Chassis and the Longitudinal Axis

$M_{longitudinal}$: Moment Around the Longitudinal Axis

$M_{lateral}$: Moment Around the Lateral Axis

$M_{vertical}$: Moment Around the Vertical Axis

$F_{lateral}$: Lateral Force

a_1 : Height of the Side Box Sections

a_2 : Width of the Side Box Sections

a_3 : Distance between the Center and the Side Plates

α : Angle between the Longitudinal Axis and the Side Plates

b_1 : Distance between the Upper Plate and the First Reinforcement

b_2 : Width parameter of the First Reinforcement

c_1 : Distance between the Upper Plate and the Second Reinforcement

c_2, c_3 : Width parameters of the Second Reinforcement

d_1 : Distance between the Upper Plate and the Third Reinforcement

d_2, d_3 : Width parameters of the Third Reinforcement

e_1	: Distance between the Upper Plate and the Fourth Reinforcement
e_2, e_3	: Width parameters of the Fourth Reinforcement
t_1	: Thickness of the Upper Plate
t_2, t_3	: Thicknesses of the Side Plates
t_4	: Thickness of the First Reinforcement
t_5	: Thickness of the Upper Part of the Second Reinforcement
t_6	: Thickness of the Lower Part of the Second Reinforcement
t_7	: Thickness of the Upper Part of the Third Reinforcement
t_8	: Thickness of the Lower Part of the Third Reinforcement
t_9	: Thickness of the Upper Part of the Fourth Reinforcement
t_{10}	: Thickness of the Lower Part of the Fourth Reinforcement
t_{f1}, t_{f2}, t_{f3}	: Thicknesses of the Stiffeners
d_{ra}	: Distance between the Rear Axle Connection Parts
X	: Set of Design Variables
$O(X)$	: Objective Function
$M(X)$	: Mass Function
$\sigma_i^{\max}(X)$	: Maximum Stress at the ith Welded Region
$\sigma_i^{\lim}$	: Limit Stress at the ith Welded Region
$P(X)$	: Penalty Function
$p_i(X)$	: Penalty Function of the ith Welded Region
r_i	: Penalty Coefficient of the ith Welded Region
$F(X)$	: Fitness Function
m^{target}	: Target Mass

ABBREVIATIONS

FEA	:	Finite Element Analysis
FEM	:	Finite Element Method
CAD	:	Computer Aided Design
ESO	:	Evolutionary Structural Optimization
LP	:	Linear Programming
NLP	:	Nonlinear Programming
GA	:	Genetic Algorithm
CAE	:	Computer Aided Engineering
IIW	:	International Institute of Welding
LEFM	:	Linear Elastic Fracture Mechanics
FAT	:	Fatigue Class

CHAPTER 1

INTRODUCTION

Earth-moving machines are heavy-duty engineering vehicles which are used for engineering projects such as roads, dams, open pit excavation, quarries, trenching, recycling, landscaping and building sites [1]. The most common types of earth-moving machines are: excavators, backhoe loaders, bulldozers, loaders, cranes, drilling machines and graders. Each of these machines has powerful engine and hydraulic system, and they are faced with high loads during their applications, so that they must be capable of working in rough conditions.

Excavator is a mobile machine which is moved by the help of either crawler track or rubber-tired undercarriage, with an upper structure capable of continuous rotation [2]. Upper structure including boom, arm, bucket and cab is mounted on a rotating platform over an undercarriage with tracks or wheels (Figure 1.1). It is primarily designed for excavating with a bucket, without movement of the undercarriage during the work cycle. An excavator work cycle normally includes digging, elevating, swinging and discharging of the material [3]. Weight of the excavators ranges in a large variety. According to their sizes and power ratings, they are used in various engineering applications with several types of attachments, like bucket, shovel, breaker, auger or grapple.
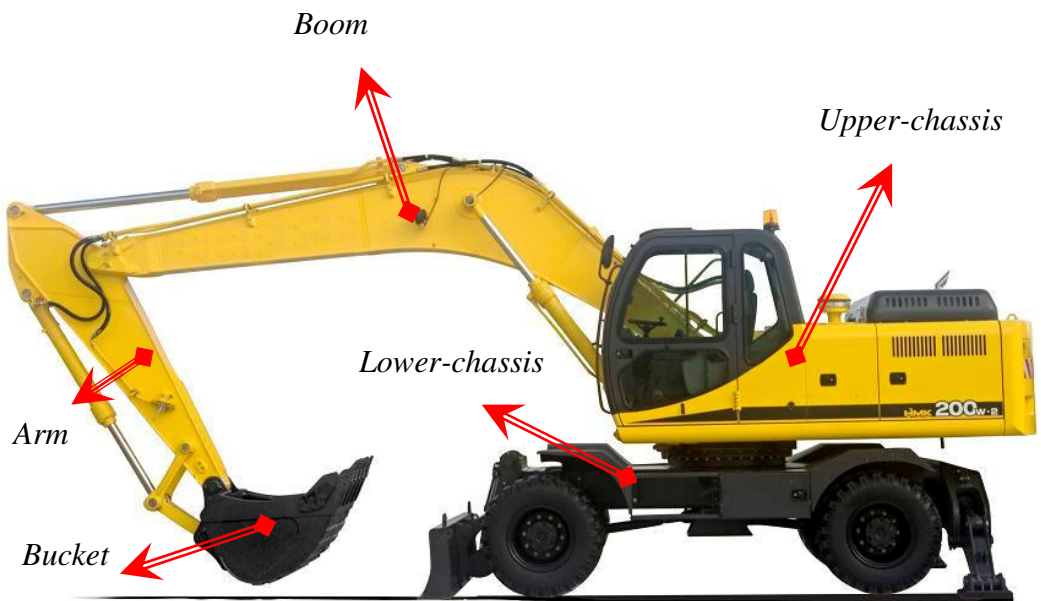
Figure 1.1 - General view of an excavator

Excavators with rubber-tired undercarriage are called wheeled excavators. Wheeled excavators come with an advantage in transportation, since they can be driven on road. Most wheeled excavators have a dozer blade for pushing removed material back into a hole [4]. Outriggers and dozer blade (Figure 1.2, Figure 1.3) are taken down by hydraulic cylinders, before the wheeled excavator starts digging.

Front and rear axles are mounted on undercarriage which is also called as lower chassis of excavator. Rear axle is fixed on the lower chassis by bolts. Front axle is connected by a hinge pin, which gives rotation freedom around the longitudinal axis (Figure 1.3). Required rotational mechanical power for the axles is transmitted by shafts from the transmission powered by a hydraulic motor. Hydraulic motor and transmission are placed under the lower chassis.
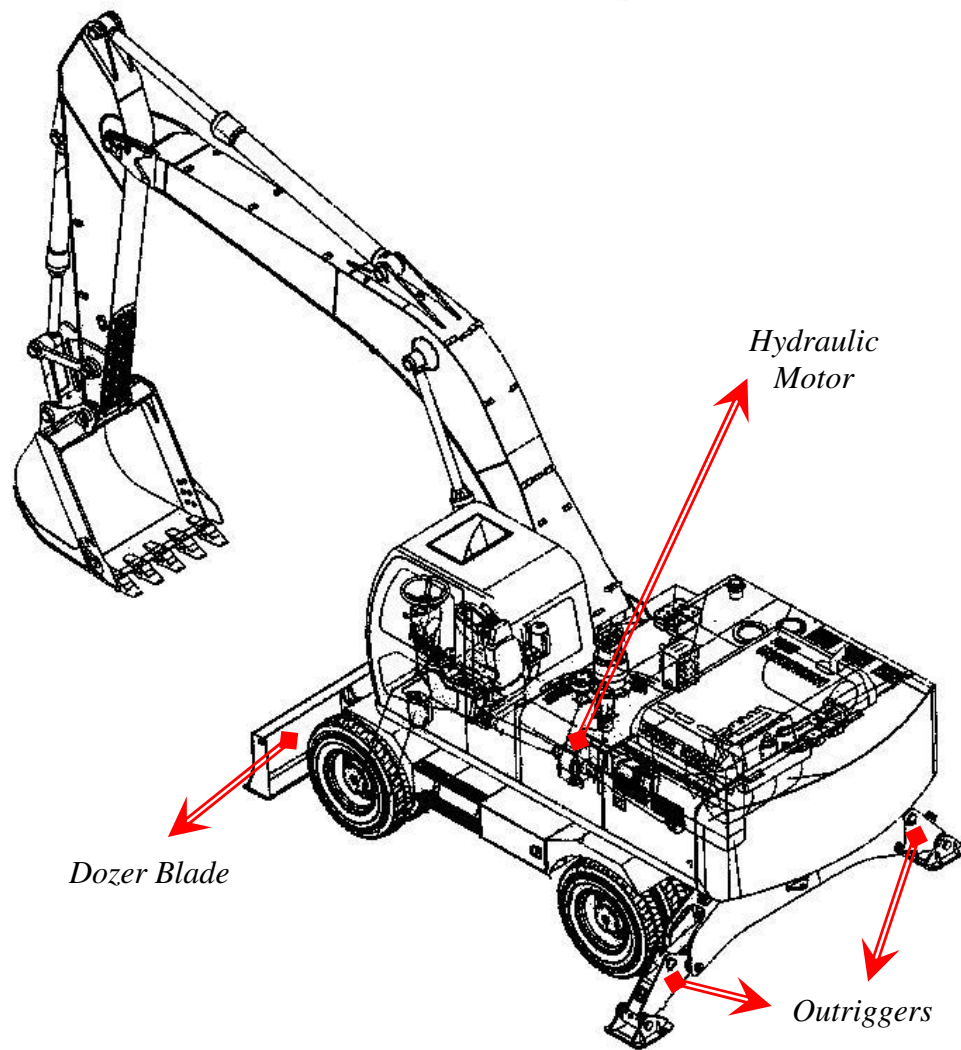
Figure 1.2 - General view of a wheeled excavator

Lower chassis is one of the main parts of the wheeled excavator. It accommodates the parts that carry other attachments, like upper chassis, dozer blade, outriggers and axles. It is constructed by welding these parts each other, which makes the lower chassis weighty and costly. Moreover, assembling and also disassembling this structure come with loss of labour force and high cost for suppliers. Therefore, the lower chassis must be strong enough to cope with severe working conditions during the whole life of the wheeled excavator. Accordingly, strength analysis becomes more important for the design of the lower chassis.

Pin connecting front axle

Outriggers

Parts connecting rear axle

Dozer Blade
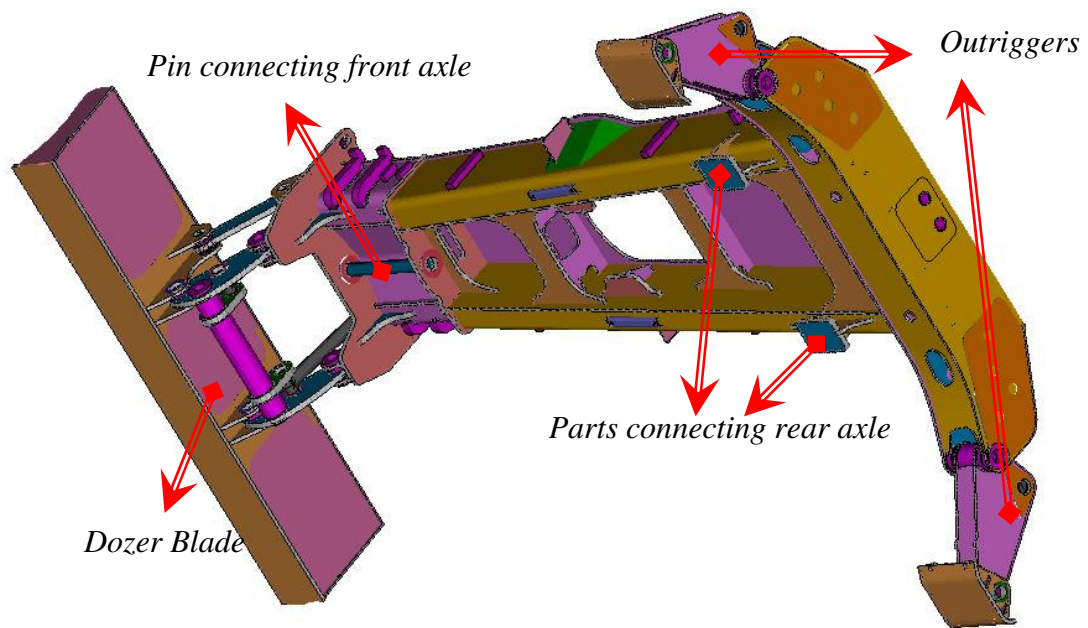
Figure 1.3 - Lower chassis of a wheeled excavator

Finite Element Method (FEM) is the most popular technique that is used for strength analysis of structures. In general, computer aided drawing (CAD) programs are used to generate the model for the finite element analysis (FEA), although the most of commercial FEM programs have a CAD interface. After generating the model, adequate mesh which defines geometry of the model is generated in a commercial FEM program. Therefore, using two different programs causes loss of time. Consequently, boundary conditions including the critical loading cases must be defined, which needs experienced engineering knowledge.

The aim of this study is to design a computer program which optimizes the geometry of the lower chassis of wheeled excavator with respect to mass and stress data obtained from FEA for a set of specified boundary conditions.

First of all, boundary conditions simulating critical loading case are determined. A program based on Microsoft Excel is performed to determine the critical loading cases for the lower chassis. In the program, arm breakout force (F_{arm}) at the bucket tip during the digging operation is calculated for varying hydraulic cylinder lengths (Figure 1.4). Since the excavation motion is slow, the inertial forces are neglected and static force analysis is performed to calculate F_{arm}. The structure is analyzed within the boundary conditions defined by the program with different excavating positions. Two of the critical loading cases are chosen as design criteria.

F_{arm}
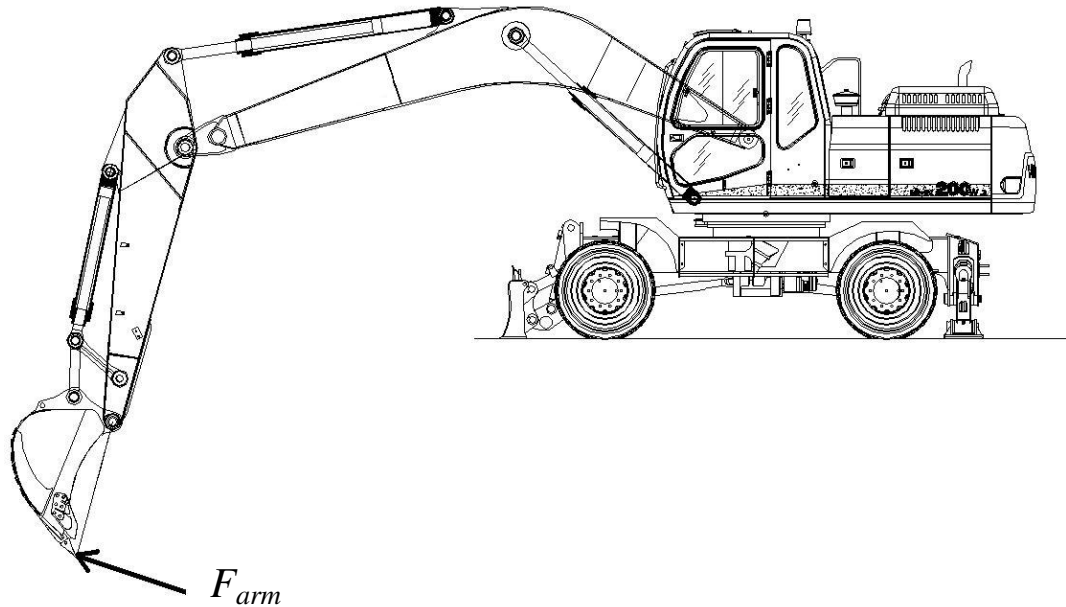
Figure 1.4 - Arm breakout force

Secondly, another program based on Microsoft Excel is performed to compute all necessary data that is required to generate the model with varying shape parameters in a commercial FEM program, so that it is not needed to use an another parametric CAD program. MSC. Marc Mentat, which is a commercial FEM program, is used to perform FEA of the lower chassis.

Finally, Smart Designer which is an optimization program developed by Cevdet Can Uzer is implemented into the program [5]. Smart Designer is performed to optimize the excavator boom geometry using Genetic Algorithm which is a heuristic method. Fitness functions are generated with respect to the stress and mass data obtained from the output of FEA. The parameters of the fitness function are redefined for the lower chassis of wheeled excavator.

CHAPTER 2

LITERATURE REVIEW

Optimization means the study of problems in which one seeks to minimize or maximize a function by changing the values of variables within a determined region. It is a powerful problem solving methodology and is widely used for different types of applications in management science, industry and engineering to minimize the cost and maximize the profit. Optimization becomes more popular in engineering design, since the majority of a design engineer's work concentrates on improving existing system [6].

2.1 Structural Optimization

Structural optimization is a type of optimization problems including objective function(s) and constraints that are based on structural analyses. It can be symbolically formulated as [8];

Minimize $\quad f(x)$

Subject to $\quad g(x) < 0,$

$\qquad\quad h(x) = 0,$

$\qquad\quad x \in D,$

where x denotes a design variable, f(x) is an objective function, g(x) and h(x) are considered as constraints, and D is the domain of the design variable.

2.1.1 Sizing Optimization

Sizing optimization parameters include the geometric parameters of the structure [6]. As can be seen in Figure 2.1, cross-sectional geometry and plate thickness are some examples of sizing design variables. The global geometry of the structure does not change, during the sizing optimization iterations. This means that remeshing of the whole geometry is not required, which is an advantage to decrease the process time of the optimization [8].
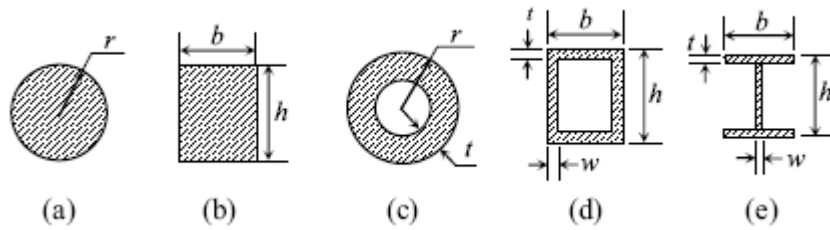
Figure 2.1 - Sizing design variables for cross-sectional areas of truss and beam [6]

2.1.2 Shape Optimization

Boundary of the product geometry can be changed in shape optimization with varying parameters. Some examples of shape optimization variables are shown in Figure 2.2. Since the geometry of the structure changes during the optimization process, finite element model of the structural domain must be regenerated by

remeshing [8]. Therefore, shape optimization problems are more difficult to solve than the sizing design problems [6].
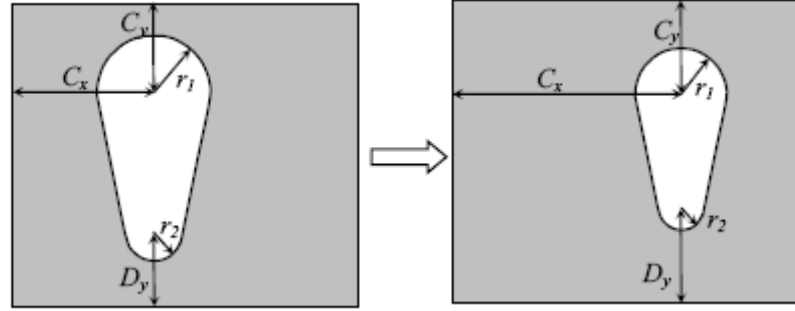
Figure 2.2 - Shape Optimization Variables [6]

2.1.3   Topology Optimization

The third optimization technique is topology optimization. Early studies in topology optimization focused on truss structures. For a set of points in a determined space, design engineers used topology optimization to connect these points with truss structures [6]. Recent studies in topology optimization generally utilize finite element analysis (FEA). Evolutionary structural optimization (ESO), which is developed by Xie and Steven [9], is one of topology optimization techniques using FEA. Removing inefficient material from a structure forms the main idea of ESO. The element removal criterion is usually based on the element Von Mises Stresses [10]. Inactive material elements of structure are removed until a determined rejection criterion is reached. In Figure 2.3, a spanner design formed by ESO is shown.
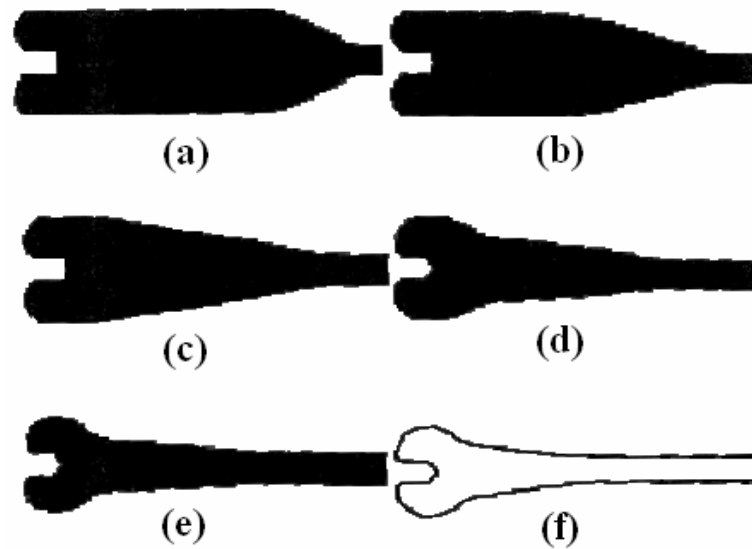
Figure 2.3 - Evolution of a spanner and final shape [9]

2.2   Optimization Algorithms

Optimization problems are considered in two main titles which are linear programming (LP) and non-linear programming (NLP) with respect to their analyses types. LP problems include the optimization of linear objective function and a series of linear inequality and equality constraints. Most of structural optimization problems are based on NLP because of their objective functions including non-linear equations.

Today's structural optimization problems are very complicated and include high number of design parameters. It is difficult to set an exact optimization algorithm for these types of problems, so that Heuristic Algorithms are widely used by design engineers. Structural optimization problems generally include high number of local optimum solutions. These algorithms do not usually guarantee performing the global

optimum of the problem. However, a difference of 1% or less between qualities of a near optimum solution and the global optimum is usually accepted [25].

Tabu Search, Simulated Annealing and Genetic Algorithms are the most commonly used types of Heuristic Algorithms.

2.2.1   Tabu Search

Tabu Search algorithms start out at some initial configuration which is either known or preoptimized. These algorithms search in the neighbourhood of the current configuration for the best neighbourhood configuration and make a sequence of moves to find optimum points. All the sequence of the movements is stored as Tabu Search List and the move leading back is forbidden. If the algorithm reaches the local minima or maxima, the movement to the best neighbourhood is allowed to reach global optimum [25].

2.2.2   Simulated Annealing

Simulated annealing is an iterative search method influenced by the annealing of metals [26]. The algorithm starts with an initial solution. The direction of search is controlled by a parameter called temperature. Initially, the temperature is high and the search is almost random. Then, the temperature is decreased with a cooling parameter and random movements in the search are restricted. At last, the search accepts only good movements when the value of temperature is zero.

2.2.3 Genetic Algorithm

Genetic Algorithm (GA) is an evolutionary search method inspired by natural genetics. It regenerates population of solutions to an optimization problem evolving toward better solutions by using techniques that are influenced by evolutionary biology like mutation, selection and cross-over. GA does not require detailed information about the physics of the optimization problem. So that it can be easily implemented into many types of applications in different fields such as bioinformatics, economics, chemistry, engineering.

2.2.3.1 Terminology

GA have a terminology inspired by evolutionary biology. These terms are explained in following paragraphs [27].

Population : A population is a collection of individuals that can be on anywhere of the search space.

String : In an optimization problem, a string is a possible solution which is an individual of population. It can be in form binary or real numbers according to the type of the optimization problem.

Gene : Each parameter in a string is called as a gene. As it is mentioned before, gene can be defined by real or binary numbers.

Fitness number : Fitness number is a value that defines the goodness of a string in the population.

2.2.3.2   Genetic Operators of Basic Genetic Algorithm

First of all, many solutions are performed to generate an initial population. The population size varies with respect to the type of the optimization problem. In general, the first population is generated randomly at the beginning of the optimization. However, the initial population may include pre-optimized individuals. The fitness value of every individual in the population is evaluated. Individuals are selected according to these fitness numbers to generate next population during the each iteration of the algorithm. The next population is generated by applying reproduction operators, crossover and mutation, on selected solutions. Parents are selected for each solution and new children are produced. This process is continued until the new population size becomes appropriate. Then, the fitness values are evaluated again and the algorithm runs in a loop. In general, it is stopped when the termination condition is satisfied. The flow chart of the algorithm is shown in Figure 2.4.

A basic Genetic algorithm includes four main genetic operators. These are evaluation, selection, crossover and mutation.

Evaluation

At evaluation stage, each individual in the population is evaluated by the fitness function and given a fitness number. Then, it is possible to arrange the individuals in the population in order to strongest to weakest. Only in this stage GA uses information about the problem itself.
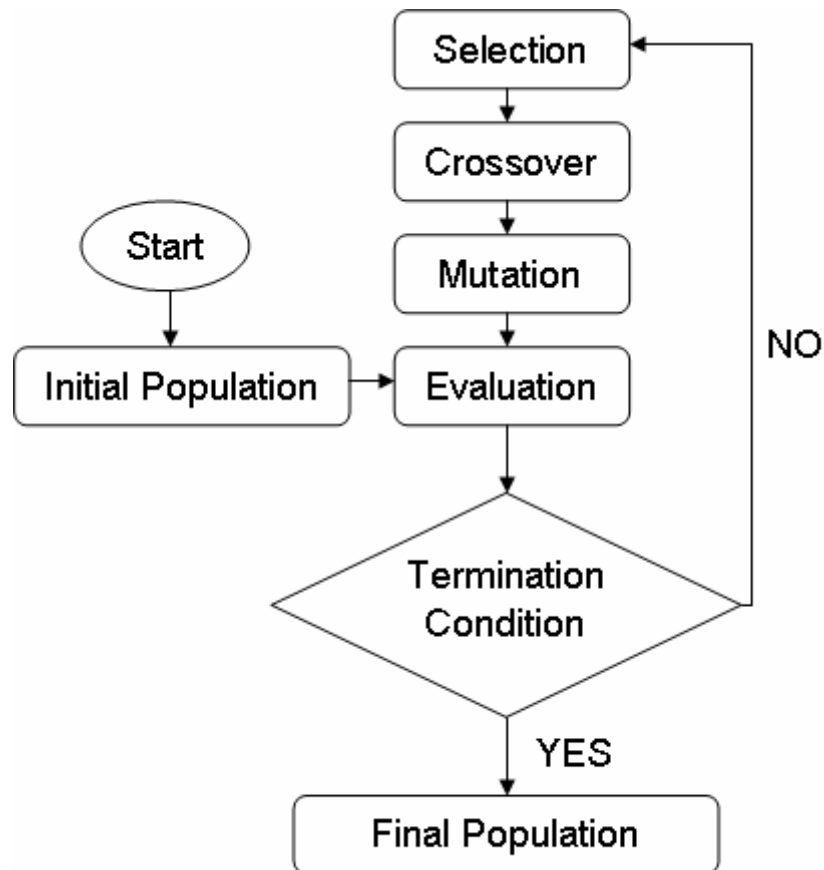
Figure 2.4 - Flowchart of a basic genetic algorithm

Selection

At this stage, some of the individuals in the population are selected according to their fitness numbers for crossover. As it is expected, stronger individuals have more chance to survive in the population. There are many different methods for selecting individuals to be used in the next process of the algorithm. The most popular one is roulette wheel selection method [27]. The fitness number is used to calculate a probability of selection for each individual. Each individual has a slot in the roulette wheel according to the probability value which is calculated by using fitness number. Then, the roulette wheel is rotated and one of the individuals in the population is selected for reproduction. The individuals may be selected more than once. An intermediate population is formed with selected individuals.

Crossover

Next generation is formed by coupling the individuals in the intermediate population randomly. Two new children are formed by crossing over each couples' genes. Crossover operation may differ according to the representation method of strings. The strings may be in binary or real format. If binary representation is used, crossover is done by exchanging the genes from randomly selected or determined sections of the string. If real number representation is used, a weighted mean funtion is used to calculate the value of the new gene.

Mutation

Mutation is used to maintain genetic diversity in the population. GA sometimes converges to a local optimum. To avoid this problem, randomly selected genes are implemented into the strings in the population. There is a parameter which defines the ratio of mutation. It must be determined meticulously to control the evolution of generations.

2.3   Previous Works on Structural Optimization

Conle et al. [19] explained a brief history of the evaluation of fatigue analysis software in the automotive, truck and earth-moving machinery industries. First of all, the main idea behind using computer aided engineering (CAE) is to reduce numbers of prototypes and shorten the design cycle time. It is stated that fatigue problems are based on three main subjects: material properties; the effects of geometry; and the loadcases. Theoretical observations are made for change in material properties after tensile plasticity. Generated formulations are implemented in fatigue analysis programs to produce the stress and the strain history. Fatigue analysis has been made

generally with uniaxial deformation models. However, developments in computer technology enabled storing long histories from strain and load channels. Furthermore, the improvements of the program logic enabled implementing the multiaxial models in fatigue analysis packages. Another important issue in the vehicular industry is the measure of fatigue life with respect to the stress strain data obtained in the structure. The various commercial packages use different types of parameters including Von Mises equivalent stress to calculate fatigue life. Previous studies on fatigue analysis showed that both normal and shear stress must be utilized on the critical plane to get more accurate results. Also, the study of Sonsino et al. [20] presented the importance of principal stress direction in laser beam welding which is widely used in automotive industry.

Secondly, FEA is used to perform load vs. strain diagram within the structure geometry. In general, fully elastic FEA models are generated because of the expense and the general poor quality of FEA plasticity models. Then, a plasticity correction factor is applied to simulate the behaviour of the material in a better approximation. On the other hand, boundary conditions are very important in FEA. It is very difficult to select a single critical loadcase, as complexity of FEA models expands through years. Therefore, a large number of different loadcases must be checked. The unit-load superposition approach is implemented and all the loadcases are solved for all the elements. Finally, it is stated that problems still exist to be studied on. For instance, the effect of overloads on fatigue life requires further research to be incorporated into chassis fatigue life calculation software.

Rastogi [11] worked on lay-up optimization of an all-composite pick-up truck chassis. FEA is performed to optimize the orientations and the sequence of composite material. NASTRAN, a commercial FEA product, is used to compute fundamental modes, bending and torsional stiffnesses of the structure. A model created within NASTRAN is shown in Figure 2.5.
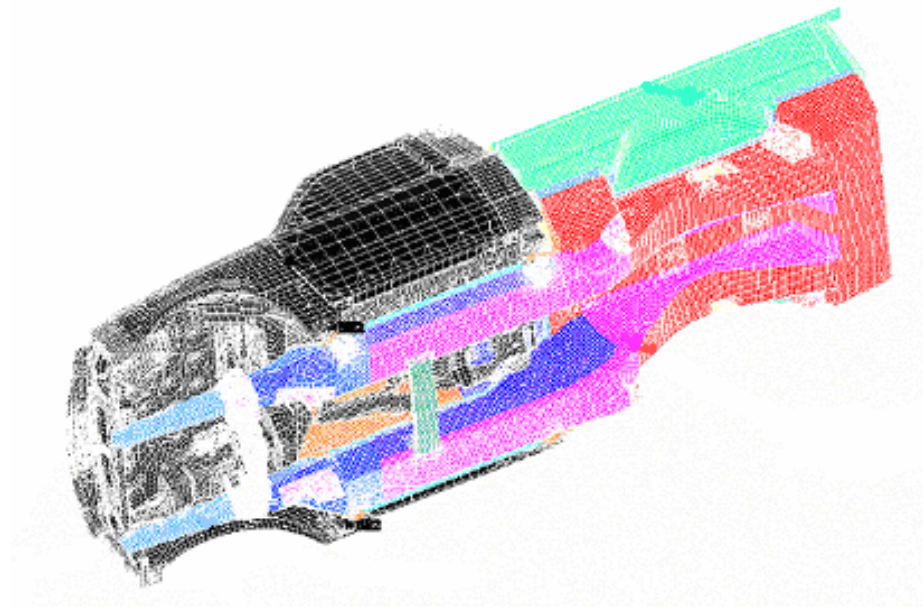
Figure 2.5 - FEA model of a pick-up truck chassis

GENESIS, which is a commercial structural optimization program, is used to find the right orientations and different carbon/epoxy materials for the six zones determined in the structure while the bending stiffness targets are exceeded. Both the initial and optimized designs are subjected to strength analysis to compute stresses and strains in the principle material coordinates. Tsai-Wu composite material failure theory is applied to predict failure in composite parts. Von Mises failure criteria is used for the metallic components of the structure. Consequently, it is stated that Von Mises stresses in metallic components and Tsai-Wu failure index in carbon/epoxy materials are less than corresponding failure criteria, for both the initial and optimized designs.

Fasel et al. [12] presented an optimization approach based on evolutionary methods for tubular motorbike-frame. The optimization objective is to minimize the mass of the frame within a given stiffness and strength constraints. Stiffness and strength calculations are performed by their own FEA program. ANSYS, which is a commercial FEA program, is used only as a pre- and pro-processor in the study. They performed a new heterogeneous genotype that allows different parameter types

17

in evolutionary optimization algorithm. Moreover, the impacts of the parameterization types are compared to each other.

Gadus [13] worked on a mass optimization of a frame of a special tractor trailer designed for transport of seeding machines. The aim of the optimization to obtain the lowest possible structure mass within allowable Von Mises stresses. Strength analyses are performed by using Pro/MECHANICA which is integrated with CAD product Pro/ENGINEER. Finally, the total mass of the structure is reduced more than 35%.

Lee et al. [14] presented a new approach using Taguchi Method in structural optimization. They generated an algorithm that automatically finds the most appropriate set of variables to minimize the number of degrees of freedom of the problem. This algorithm is implemented on Pro/ENGINEER which is a commercial CAD platform including FEM solvers. In the paper, they performed the structural optimization of a rear roll bracket which is a structure that mounts an engine on the body of a car. The first natural frequency of the structure must be maximized, so it is chosen as the objective function of the problem. CAD model of the structure and some design variables are shown in Figure 2.6. Some of design variables are put out with respect their effect on the objective function. An optimal estimate is obtained by using effective variables. Finally, objective function is improved by 48.8%.
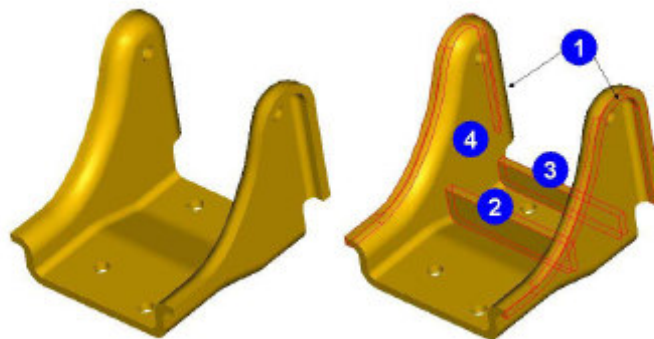
Figure 2.6 - CAD of rear roll bracket and its variables [14]

In an another study of Lee et al. [15], Taguchi method is applied again to optimize the boom structure of an excavator. One of the most critical excavation position is chosen as the loading condition for FEA of the structure. They model the excavator boom mostly with quadrilateral shell elements. The other parts of the structure are modelled by beam elements. The objective function is utilized to minimize the volume where the maximum Von Mises stress value does not exceed the predetermined value. The design variables are shown in Figure 2.7. There are totally 13 parameters that determine the geometry of the structure. The problem is solved after 22 iterations and 639 FEM runs. The volume of the structure is reduced by 0.004 m^3 and the maximum Von Mises stress on the boom is reduced from 256 MPa to 212 MPa. The stress distributions of the initial and optimized booms are shown in Figure 2.8.
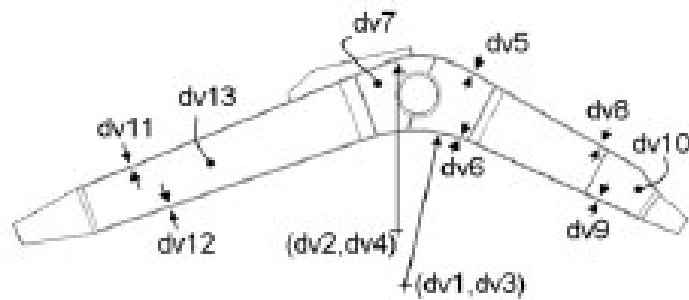
Figure 2.7 - Design variables of excavator boom [15]
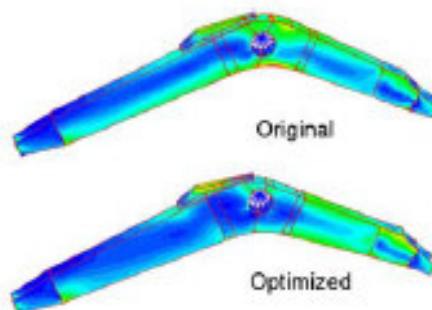
Figure 2.8 - Stress distribution of excavator boom [15]

In the thesis study of Yener [21], a computer interface called OPTIBOOM is designed to perform FEA of an excavator boom automatically to find the optimum design in terms of stresses and mass by changing specified shape variables. There are six main parameters that generate the boom geometry. Also, the thicknesses of sheet metals can be changed within a predetermined range. The strength analyses of the generated booms are made under determined critical boundary conditions. Finally, maximum Von Mises stress in the boom is reduced by 21.5 %, although mass of the boom increased only by 3.6 %. In this study, optimum design depends on the user and it is not an automatic process. In the thesis study of Uzer [5], a logical optimization algorithm is implemented to OPTIBOOM. Genetic algorithm which is a global heuristic search strategy is chosen to search different boom models and achieve the optimum geometry of the boom. Objective function of the problem includes the terms of mass and Von Mises stress. It is tried to be minimized by changing geometrical variables within a predetermined range. Finally, a boom geometry which is 4.6% lighter than the initial design was performed while the design stress criteria is satisfied.

Hai-jun et al. [16] worked on the structural optimization of high-speed centrifugal rotors that are used by medical, bio-industrial and bio-processing communities. Since rotors work at high rotary speeds, they can also be dangerous instruments if any structural failure occurs. The structure is modelled in a commercial FEM program, MSC. NASTRAN. The solid model is generated by using ten-node tetrahedral elements. The mesh of the model is finer around rounds and cavities. Angular velocity is applied to the elements of the model, which simulates the rotor bursting speed of 44,880 rpm. The FEA of the problem is solved under this loading condition. The structural optimization is obtained to minimize the maximum stress values at two critical regions. The maximum stress at the round and the top edge of the cavities are reduced by 31 MPa and 16 MPa, respectively. In Figure 2.9, the effect of the optimization over the shape parameters are shown.
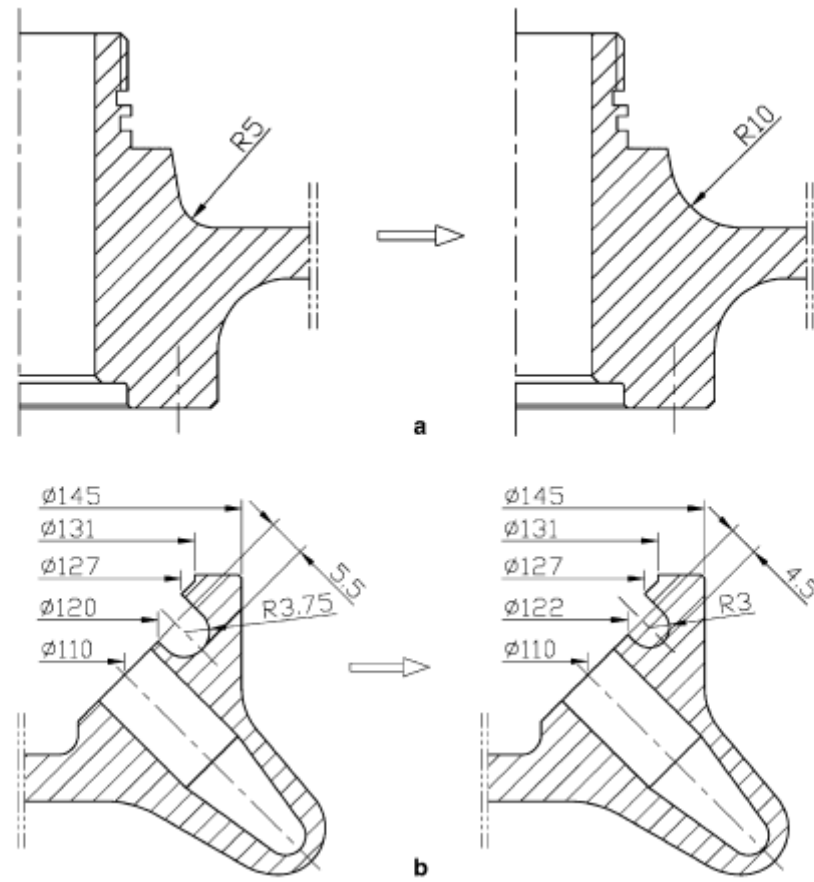
Figure 2.9 - Effect of structural optimization at two regions [16]

Martinsson [17] worked on the complex welded structures in his doctoral thesis. The aim of his study is to find out an appropriate procedure for a better optimization of complex fatigue loaded welded structures. The different fatigue design methods which are proposed by the International Institute of Welding (IIW) have been investigated and applied on an experimental structure. The stress distribution over the welded structure was computed by using FEA. Fatigue tests of the experimental structure are made to perform the accuracy of the life prediction methods. The advantages and disadvantages of Linear Elastic Fracture Mechanics (LEFM) approaches using FEA solutions were examined. Based on these investigations an automatic 3D FEM based LEFM program was performed.

Das et al. [18] presented a modified ESO algorithm using fracture mechanics methods for shape optimization of structures. The geometric model of the structure is built in FEMAP. FEA is applied to evaluate the stress distribution over the geometry by using a commercial FEM program, NE-NASTRAN. The stress intensity factors are calculated for imaginary cracks which are located along the entire structural boundary. The stress intensity factor of each crack is compared with the predetermined reference value. If it is below the reference value, an element is removed from the structure, which creates the main idea of ESO. In the study, this is performed by reducing the Young's modulus of the element to a very small value so that it has no effect on the structure. Iterations and removing material procedure are continued until convergence is achieved. The boundary elements of the final iteration are connected by a spline to perform a continuous smooth boundary. Firstly, the developed ESO algorithm is performed on the problem of shape optimization of a hole in a rectangular plate under biaxial loading. The maximum stress intensity factor is reduced by 3.3%. The distribution of the stress intensity factors over the optimized boundary is almost uniform. Secondly, the developed methodology was applied to the problem regarding the shape optimization of shoulder fillets. The maximum stress intensity factor is reduced from 12.4 MPa.m$^{1/2}$ to 9.08 MPa.m$^{1/2}$ and the results are compared to those obtained by another biological method in previous studies.

In the thesis study of Barton [23], ESO was used to optimize the milk crate design. The material volume is minimized, while the milk crate satisfies strength properties against both collapse and carrying loads. The main objective of minimizing the material volume is based on two environmental issues. Firstly, the amount of plastic entering the environment is reduced. Secondly, the energy of the transporting the product is reduced, since the weight of the crate is decreased. Small volumes of material are removed from a finite element model by using ESO. STRAND6 was used as FEA program. In each iteration, a determined fraction of the elements with the lowest Von Mises stress are removed. Since the crate is symmetric about two axes, only one-quarter of the model was generated. Three critical load cases are

chosen to simulate collapse of the crate and handle carrying condition. These boundary conditions are shown in Figure 2.10. Finally, 13% of weight was saved and the Von Mises peak stress was reduced from 3.8 MPa to 3.1 MPa.
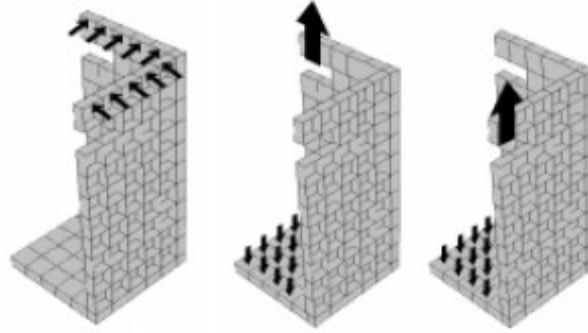
Figure 2.10 - Selected load cases include the collapse and handle carrying loads [23]

In the paper by Karaoğlu et al. [22], stress analysis of a truck chassis with riveted joints was presented. The commercial package ANSYS was used to perform FEA of the structure. The main objective of the study is to reduce the magnitude of stress near the riveted joints on the chassis frame. The parameters of side member thickness, connection plate thickness and connection plate length were varied to achieve optimum design. The Von Mises stress distribution on connection plates and side members of the chassis was presented for each variation of plate and member thicknesses. The effects of the thickness variables on the stress distribution were examined in the study.

Tekkaya et al. [24] worked on a parametric study that implementing biological growth method to a "plate with a hole problem". The optimization problem is to minimize the Von Mises peak stress on the surface by changing the geometry of the domain. Only one-quarter of the model was generated and it was run by the commercial finite element code, MARC. The effects of the optimization parameters on the problem are presented and discussed. Finally, it is stated that the method primarily performs an optimum solution for fatigue and fracture failure, since it reduces stress peak along the optimization boundary.

CHAPTER 3

FINITE ELEMENT ANALYSIS

Finite element method is widely used for the strength analysis of complex structures in earth moving machinery. The lower chassis of the wheeled excavator is modelled and the finite element analysis of the structure is performed by using the commercial program, MSC. Marc Mentat.

The main structure of the lower chassis is manufactured by welding sheet metals. Shell elements are used to simulate sheet metal in the structure. Adequate geometric properties of shell elements are defined with respect to the thickness of the sheet metal which is simulated. The cylinders actuating the dozer blade mechanism and the outriggers are modelled by using line elements in the program. The second moment of inertia and the cross-section area values of the cylinders are specified with respect to the reference axes that are defined in the commercial FEM program.

3.1 Boundary Conditions

3.1.1 Arm Breakout Force

Excavator digger mechanism is a three-degree of freedom system. The system is actuated by three independent cylinders to get the mechanism in adequate positions

for digging operation. The cylinders are called as boom, arm and bucket cylinders (Figure 3.1).
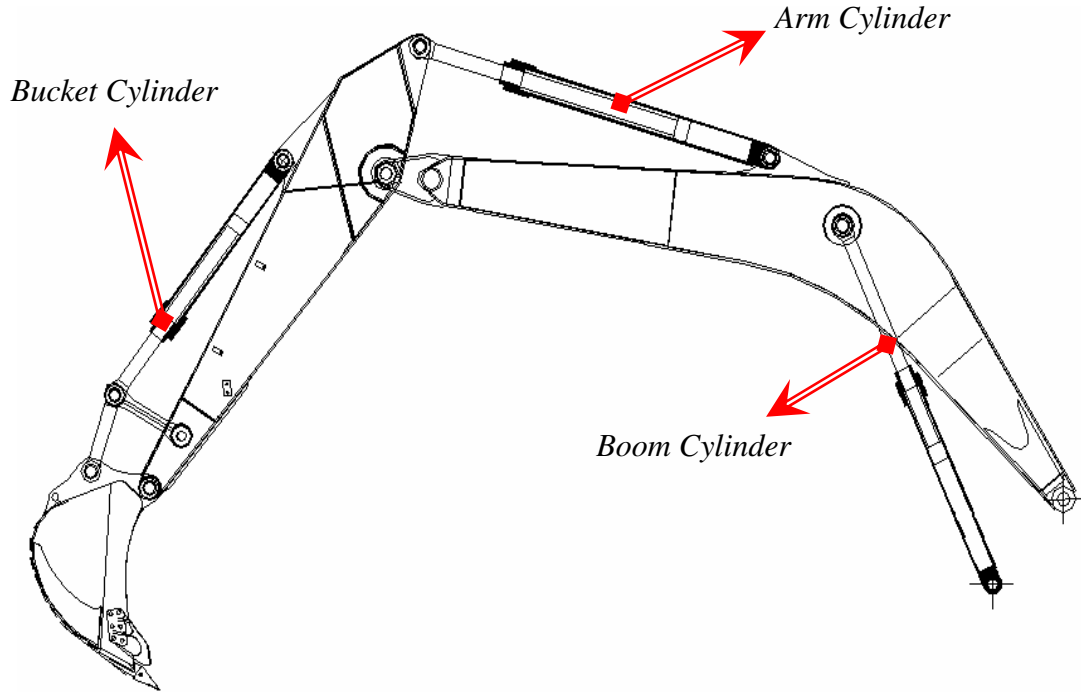
Figure 3.1 - Excavator digger mechanism

The direction and the magnitude of the forces occurring on the tip of bucket vary in a high range with respect to the mechanism position and the pressure forces in the cylinders. Since the forces are input of strength analysis of the lower-chassis, they must be calculated for different positions of the digger mechanism. First of all, position analysis of the mechanism is performed and prerequisite parameters are evaluated for force calculation. Then, the mechanism is detached to construct free-body diagrams of each part in the mechanism. The forces on the tip of the bucket and the pressure values in the cylinders are found out, after solving the system of equations based on the static force analysis of the free-body diagrams. The equations of the position and the force analysis of the mechanism were formed by the mechanical engineers in the R&D Department of Hidromek Ltd. .

Another parameter that affects the strength analysis of the structure is the position of the upper chassis with respect to the lower chassis. The angle between the longitudinal axes of the upper chassis and the lower chassis is represented as θ_{uc} in Figure 3.2. Also, the length variables of the boom, arm and bucket cylinders are shown as s_1, s_2 and s_3, respectively.
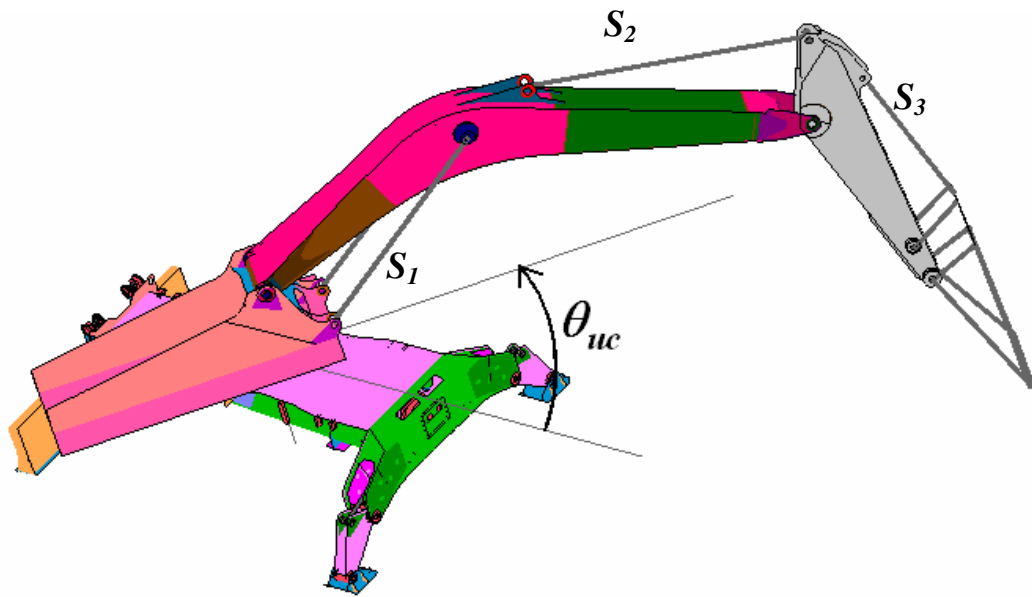
Figure 3.2 - The position of the upper chassis with respect to the lower chassis

Arm breakout forces are calculated with respect to different positions of the digger mechanism within the specified limitations. There are two main limitations on the calculation of the breakout forces. These are the pressure values in the hydraulic cylinders and the tipping of the excavator.

Firstly, when one of the cylinders is actuated with the system pressure, the pressure in the other cylinders of the excavator may rise over the working pressure. This may cause serious damage on the components like sealing elements in the cylinders and the hoses of the excavator. To avoid damage from high hydraulic pressure, anti-shock valves are placed in the hydraulic systems of excavators. It does not let the

pressure of the whole system rise over a predetermined pressure value, which is called as anti-shock relief pressure. Generally, it is adjusted to a pressure value higher than the working pressure.

The pressure values in all cylinders except the actuated one are checked whether they exceed the anti-shock relief pressure or not, while the arm and bucket breakout forces are calculated. The system is limited by anti-shock relief pressure and then the system of equations is solved again.

Secondly, some of the arm breakout forces may cause tipping of the excavator. The breakout force occurring on the tip of the bucket is checked whether it tips the excavator or not. The position of mass center of the whole excavator is found for different lengths of hydraulic cylinders and different positions of the upper chassis. The total moment of the arm breakout force and the weight of the excavator around the PQ, QR, RN and NP lines is calculated (Figure 3.3). If the values of the total moment around the specified lines are positive, the breakout force is limited with the tipping force.
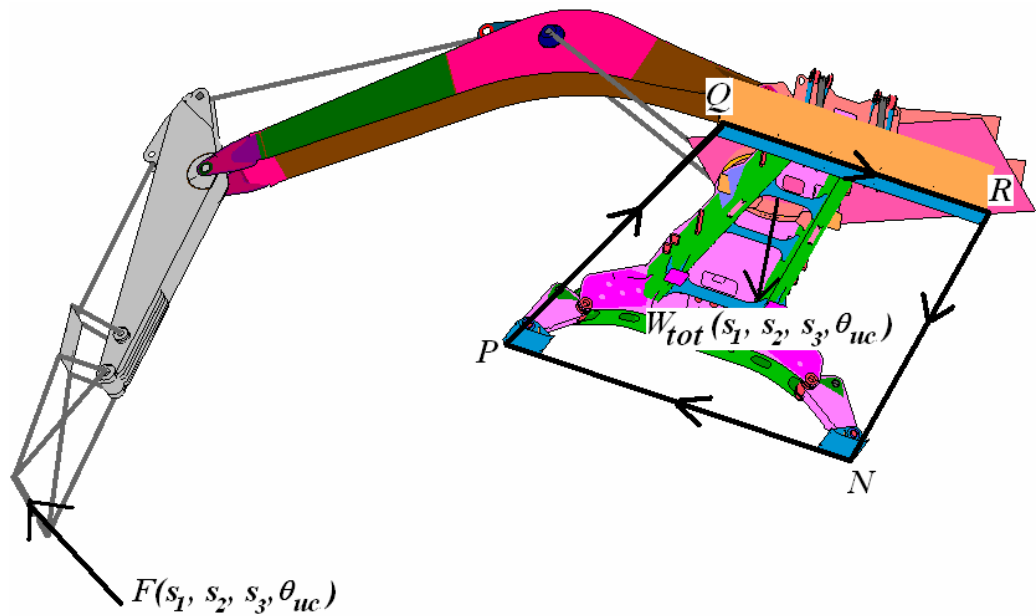
Figure 3.3 - Tipping lines of the wheeled excavator

As it is mentioned before, the excavator is capable of working in several positions by changing the specified four independent variables. To reduce the computational time, it is required to set critical boundary conditions for the lower chassis of the excavator. Also, the determined critical position must be a commonly provided condition in the lifespan of the excavator. According to these, the position of the digger mechanism which is shown in Figure 3.4 is determined as critical position by considering several positions of the mechanism and the values of s_1, s_2 and s_3 are defined.
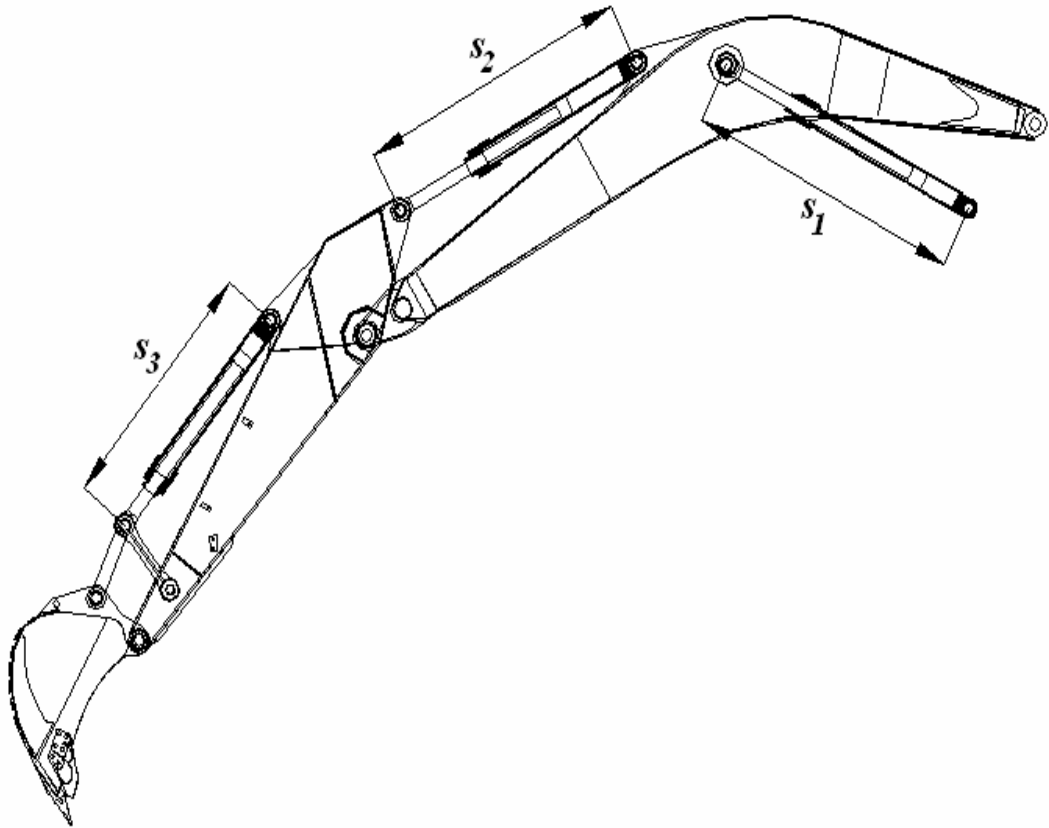
Figure 3.4 - The critical position of the digger mechanism

The arm breakout force is calculated in the determined position. The breakout force is transferred to the center of the part which is used to connect the upper chassis to the lower chassis. The forces and the moments caused by the transportation of the arm breakout force are calculated for varying θ_{uc} values. The moment values around the longitudinal and the lateral axis are highly effective on the strength analysis of the structure. The moment values are represented as $M_{longitudinal}$ and $M_{lateral}$ for varying θ_{uc} values between 0 and 2π in Figure 3.5. As can be seen in the graph, the θ_{uc} values leading high moments at the center are selected as critical. Finally, two critical load cases are defined for the FEA of the structure.
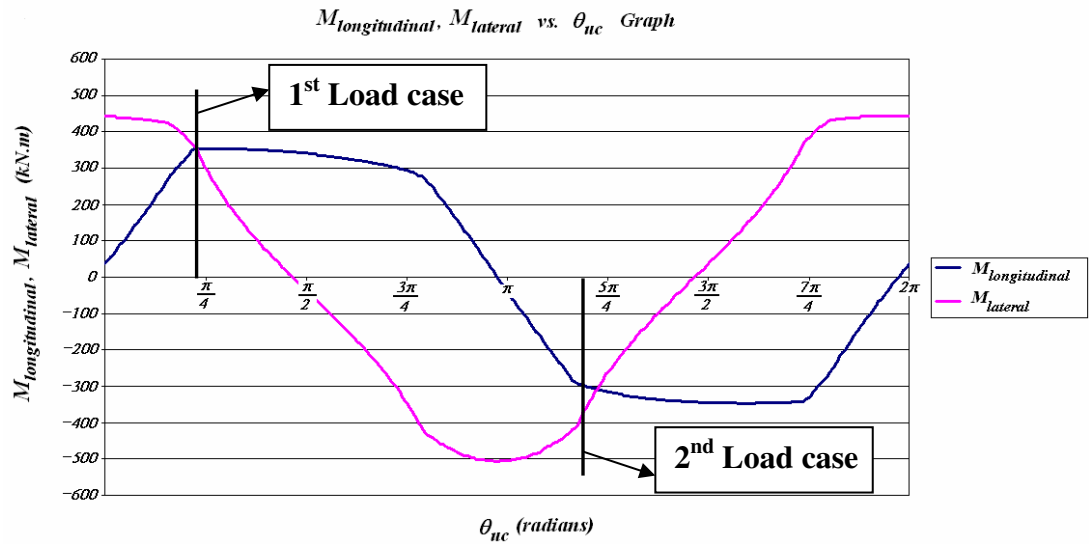
Figure 3.5 - The moment values created by the arm breakout force at the center

The center point of the connecting part is tied by link elements to transfer the point load to the upper side of the lower chassis. The link elements are shown in Figure 3.6.
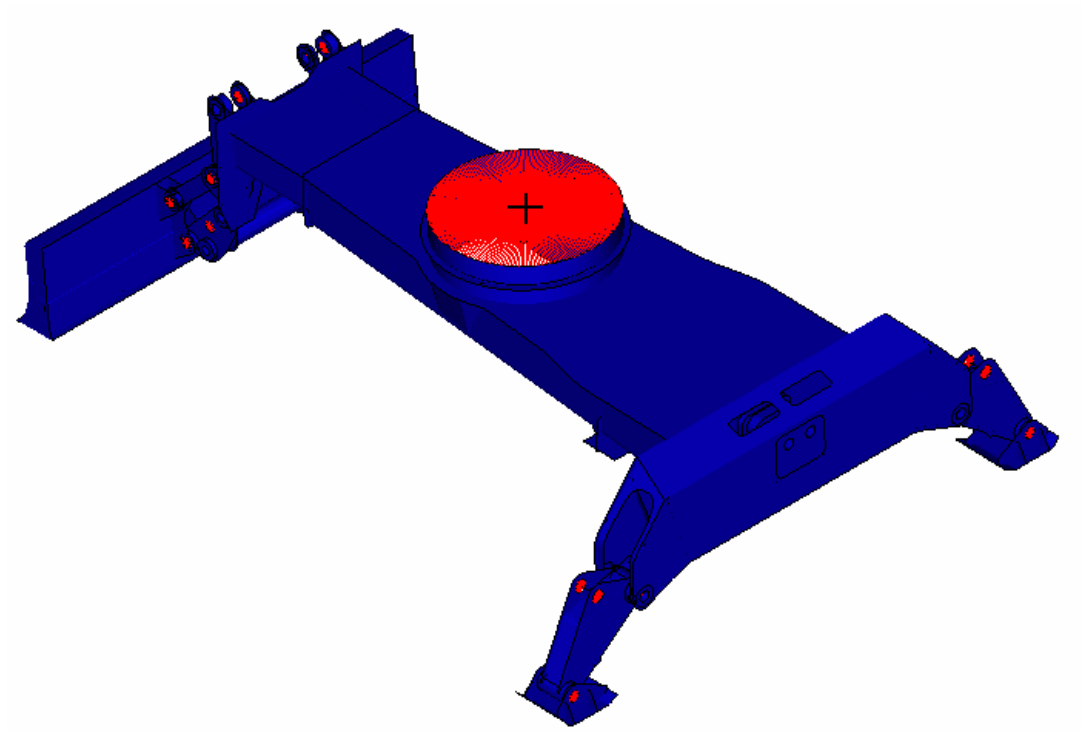
Figure 3.6 - Link elements of the FEA model

3.1.2   Lateral Force

The upper chassis of the wheeled excavator is capable of full rotation about the center of the connecting part by the help of the hydraulic swing motor. The moment created by the swing motor induces a force at the tip of the bucket. The moment generated by the swing motor and the lateral force on the bucket are represented as $M_{vertical}$ and $F_{lateral}$, respectively in Figure 3.7. $F_{lateral}$ is evaluated for the determined critical positions of the structure and transferred to the center of the connecting part.
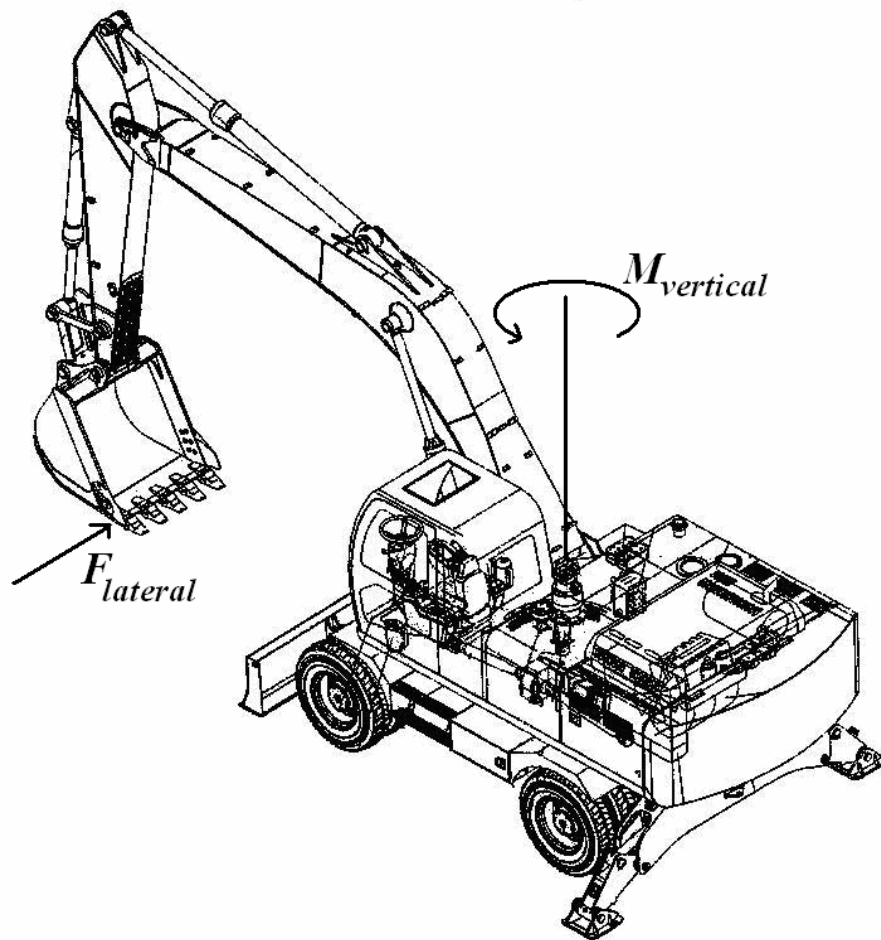
Figure 3.7 - Lateral force on the bucket

3.1.3   Gravitational Force

The center of gravity of the upper chassis including the digger mechanism is found for the critical positions of the digger mechanism. Then, the gravitational force of the upper chassis is transferred to the center of the connecting part. For the gravitational force of the lower chassis, the density of the material is defined as a material property. Then, the gravitational force is defined for each element of the lower chassis.

3.1.4   Fixed Displacement

The hydraulic cylinders of the dozer blade and the outriggers are extended until the wheels of the excavator lose contact with the ground to achieve higher breakout forces for digging. In this study, the hydraulic cylinders which actuate the dozer blade and the outriggers are fully extended. All of the nodes under the dozer blade and the outriggers are fixed in all directions.

3.2   Assumptions

Some assumptions are made to reduce the computational time and the engineering work, while the results are performed within the adequate accuracy range. The assumptions are listed as;

1. The strength analysis of the lower chassis of the wheeled excavator is performed by using FEM. So that, this study includes the assumptions based on the principles of the method which is a numerical approach to strength problems.

2. As it is mentioned before, the lower chassis is manufactured by welding sheet metals each other. However, the welding material is not simulated by using special elements in the analysis. It is assumed that the results in the connection lines of the shell elements are not accurate. So that, these results are not used in the optimization process. The stress data is collected from the regions that are the predetermined distance away from the connection lines of the welded plates. Figure 3.8 shows one of the regions where stress data is collected.
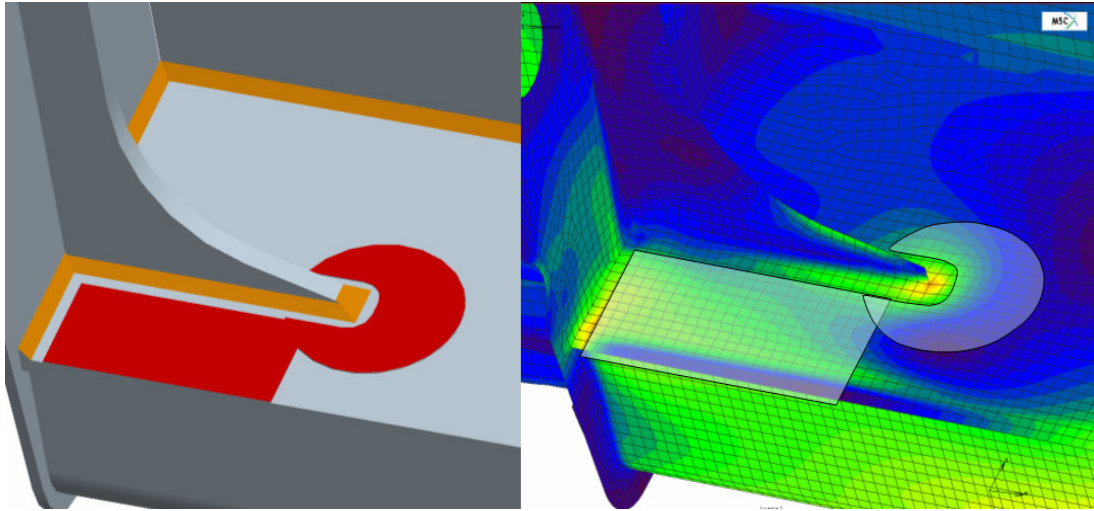
Figure 3.8 – One of the regions where stress data is collected

3. The type of the steel is the same for all the materials used in the structure. In the analysis, the material is assumed to be isotropic and homogenous. The same material properties are defined for all elements in the model. Additionally, the materials are defined as linear elastic, since the strains are very small in the analysis.

4. The axles of the wheeled excavator are not modelled in the FEA of the structure. It is assumed that the axles do not affect the results which are considered for optimization. The front axle is connected by a hinge pin to the lower chassis and the rotation of the front axle along the pin axis is not restricted. The rear axle is connected to the connection parts on the lower chassis by bolts. Another model with the rear axle is modelled for comparison. The results of the FEA do not differ so much as it is shown in Figure 3.9. The regions which are shown in circles are not considered in the optimization process.
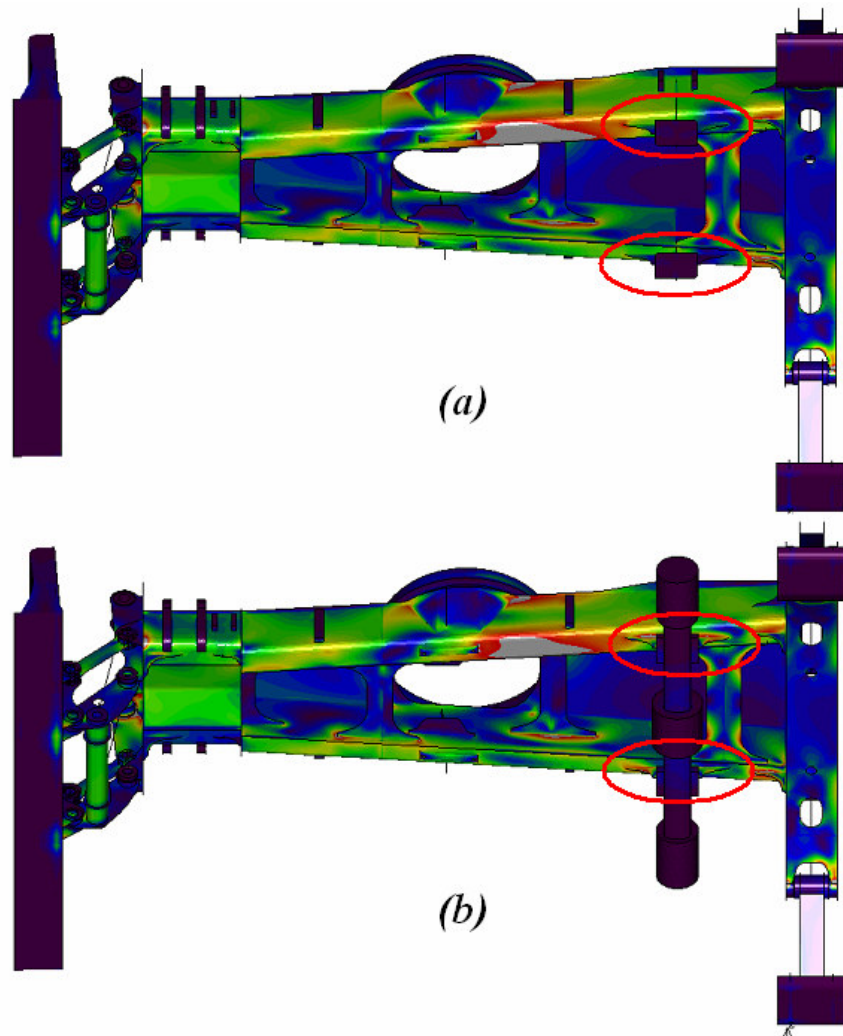
Figure 3.9 - FEA of the lower chassis (a) with rear axle (b) without rear axle

3.3 Convergence Check

The element size of the model in the finite element analysis is very important for the accuracy of the results. The model with smaller element size performs more accurate results. However, the computational time for the FEA may increase tremendously with smaller elements. Therefore, the element size must be specified meticulously to

achieve accurate results within desired computational time. The results with different element size are shown in Figure 3.10. The average element size of the models are 16 mm. and 8 mm.. The difference between the results is negligible, although the computational time increases up to 20 times. So that, the analyses are performed by 16 mm. element size.
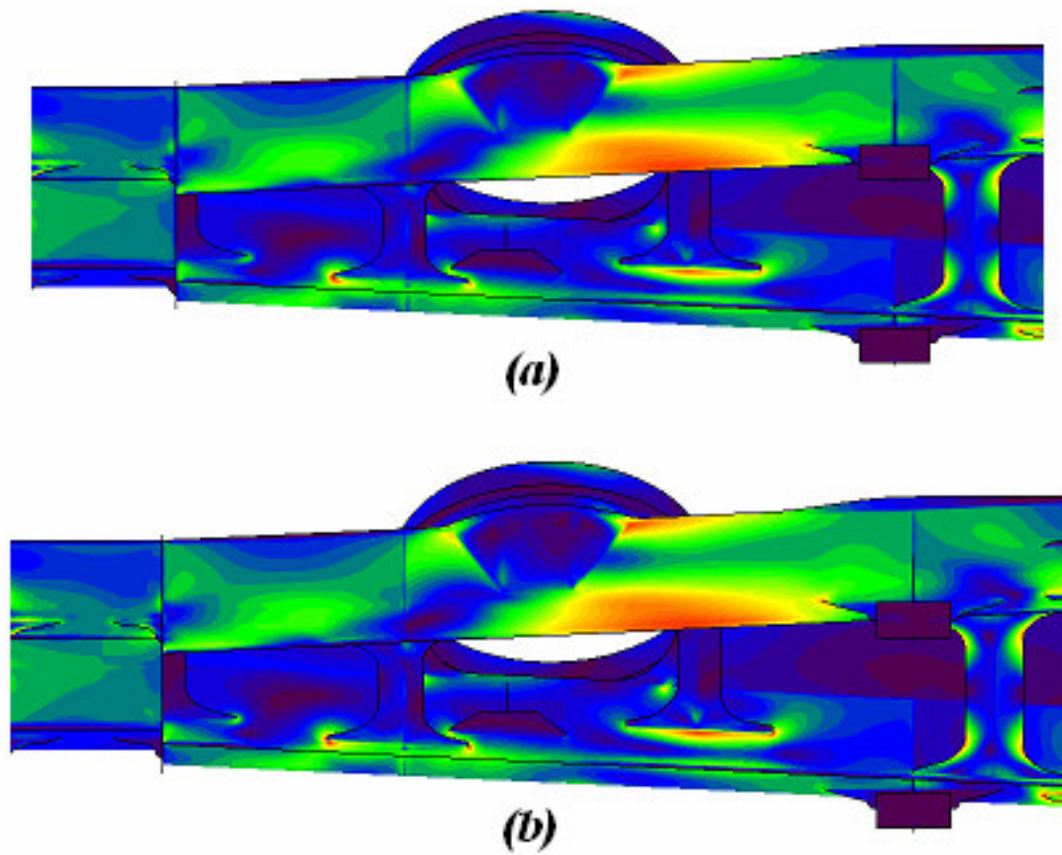
Figure 3.10 - FEA results with different element sizes; (a) 16 mm (b) 8 mm

3.4   Experimental Stress Analysis

Experimental stress analysis was performed to verify the FEA of the lower chassis of the excavator. Strain gauges are attached to the predetermined locations of the structure. Some of the gauges are shown in Figure 3.11. The rosette type strain gauges were used to reach the strain values in three different axes. The Von Mises stress values are calculated by using the strain data.

Figure 3.11 – The strain gauges used in the test

The experiment was performed in the working field of the wheeled excavator to take the digger mechanism in the specified position. The position of the mechanism is shown in Figure 3.12. The pressure in the arm cylinder is maximized and the arm breakout force is applied on the tip of the bucket.

The arm breakout force is calculated by using the force analysis of the mechanism. Same boundary conditions are set for comparison in the FEA of the structure. The percentage difference between FEA and the experimental data is shown Figure 3.13. The differences between FEA and test results are in a range of fifteen percent of the test results. The test results of only one point differ in a high range with respect to the FEA analysis. That point is under the part which is connected the dozer blade cylinder. Pin connection at that point is simulated with link elements, and it is assumed that the stress values around the pin connections do not simulate the real conditions. If the errors based on measurement, test equipments and the FEA are considered, the difference ratio between the results is satisfactory.
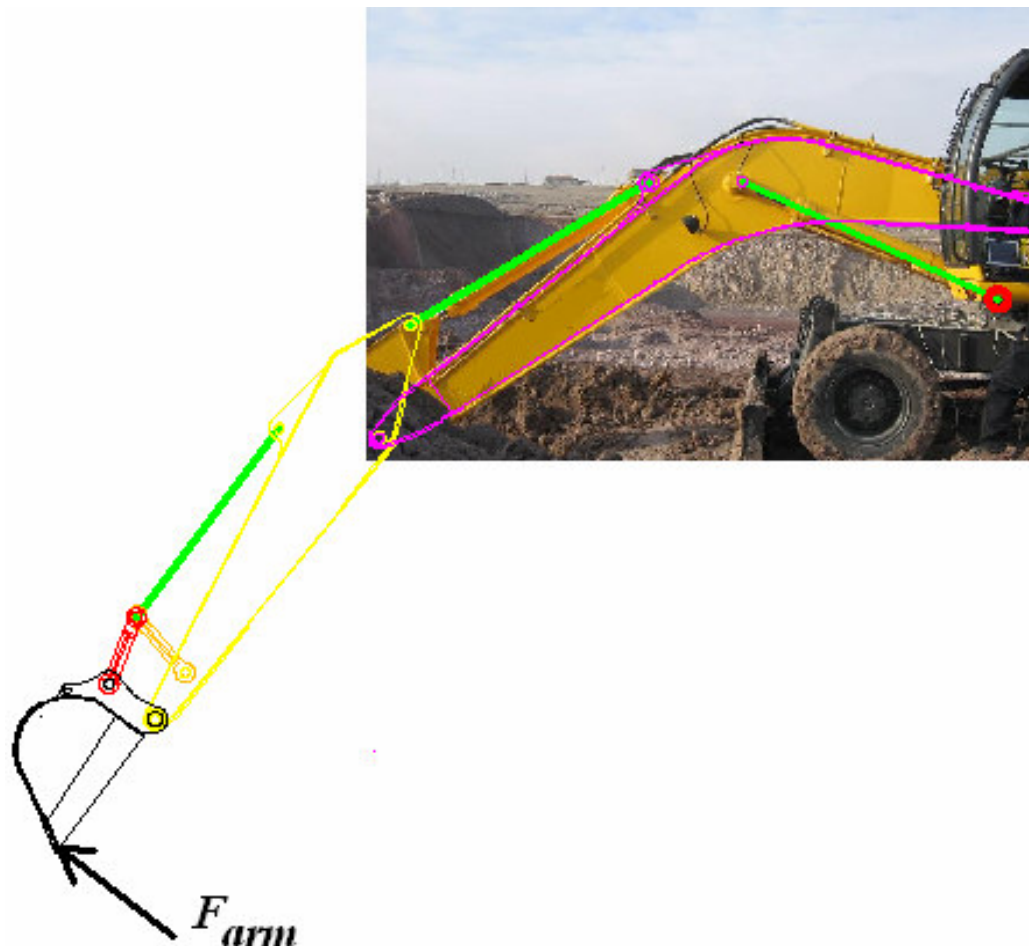
Figure 3.12 – The test position of the excavator
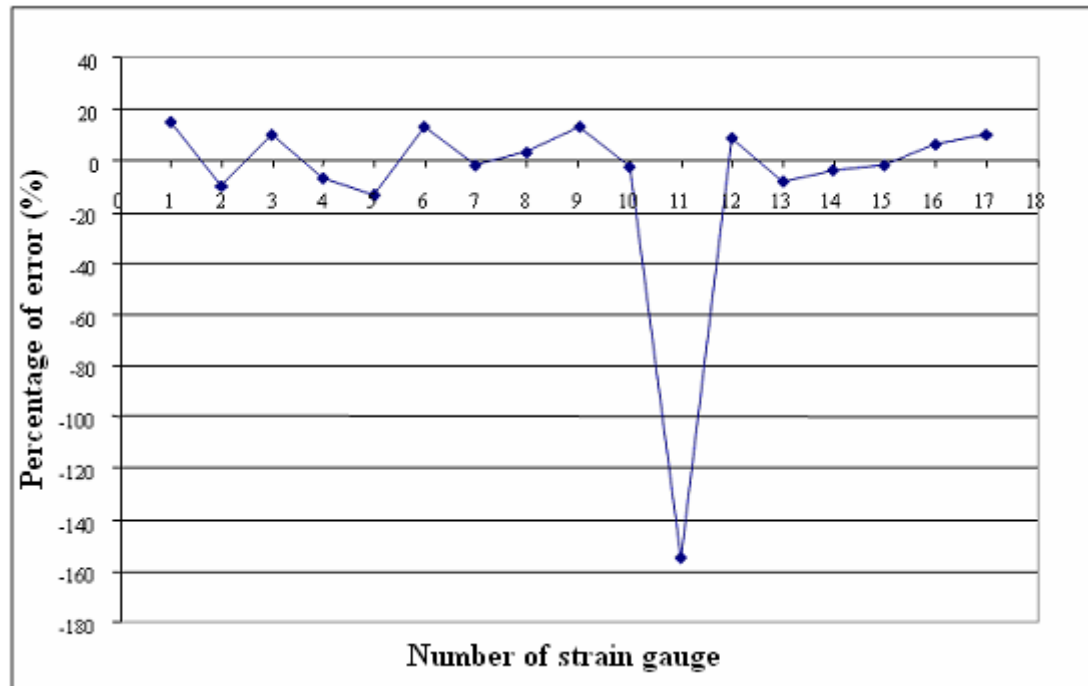
Figure 3.13 - The difference ratio between the experimental and FEA results

CHAPTER 4

PARAMETRIZATION OF THE LOWER CHASSIS

For the optimization process, finite element analyses of the lower chassis with different geometries must be performed rapidly. A computer program which generates the finite element model of the structure with varying parameters has been developed. This study especially concerns the middle part of the lower chassis (Figure 4.1). Because the middle part constitutes the main geometry of the structure, and the other parts contain many parameters and details. These details can not be examined properly with the modelling method of this study. Therefore, middle part of the structure is defined by a certain set of variable parameters while the other parts of the structure are unchanged.
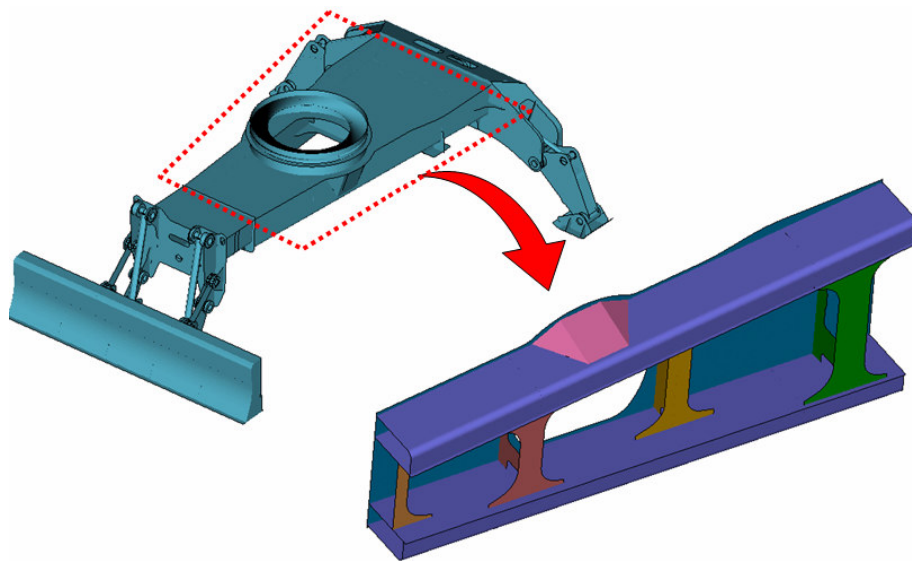
Figure 4.1 - Middle part of the lower chassis

4.1 Geometrical Parameters

The middle part of the lower chassis is manufactured by welding sheet metals with different geometric properties. Firstly, a bended plate is welded to a flat sheet metal to form the box section of the side sections of the lower chassis. The geometric parameters of the box section are represented as a_1 and a_2 in Figure 4.2. The side sections are welded to the upper plate with an angle which is represented as α. The distance between two plates is defined by a_3. Since the finite element model is generated by using shell elements, the mid-planes of the sheet metals are taken as reference. The basic parameters are selected as variables to reduce the optimization time. For instance, the bending radius is taken as constant for all models.
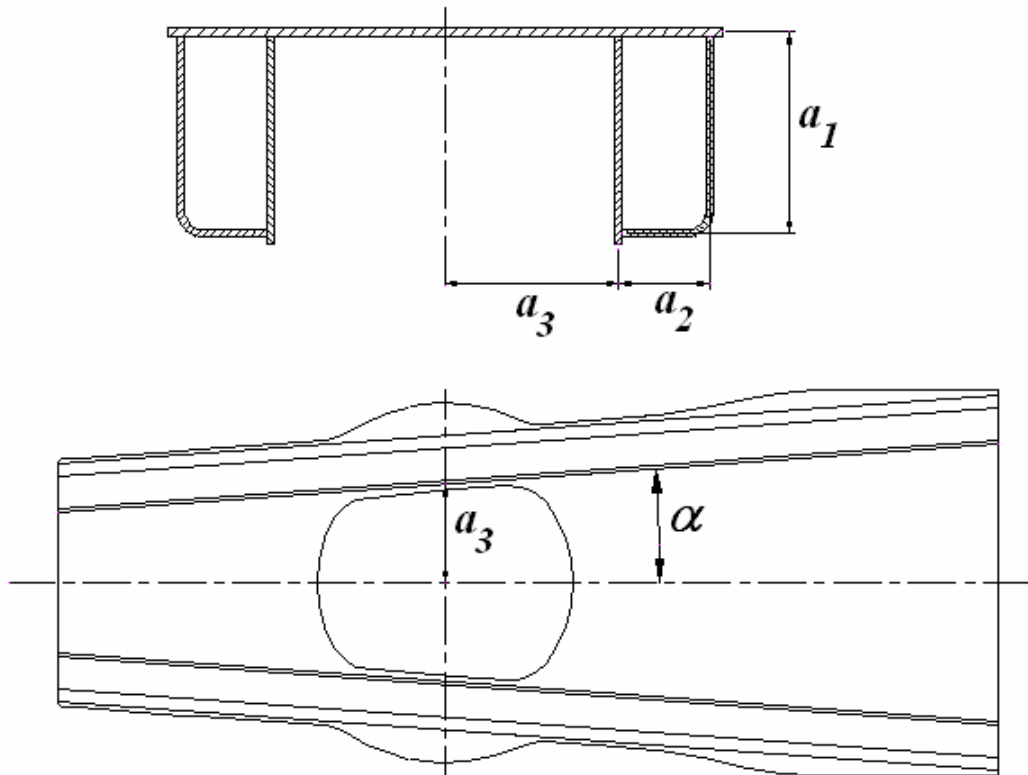
Figure 4.2 - Geometrical parameters of the side sections

Secondly, the reinforcements are welded between the side sections. There are four reinforcements under the lower chassis. The reinforcements are shown in Figure 4.3.
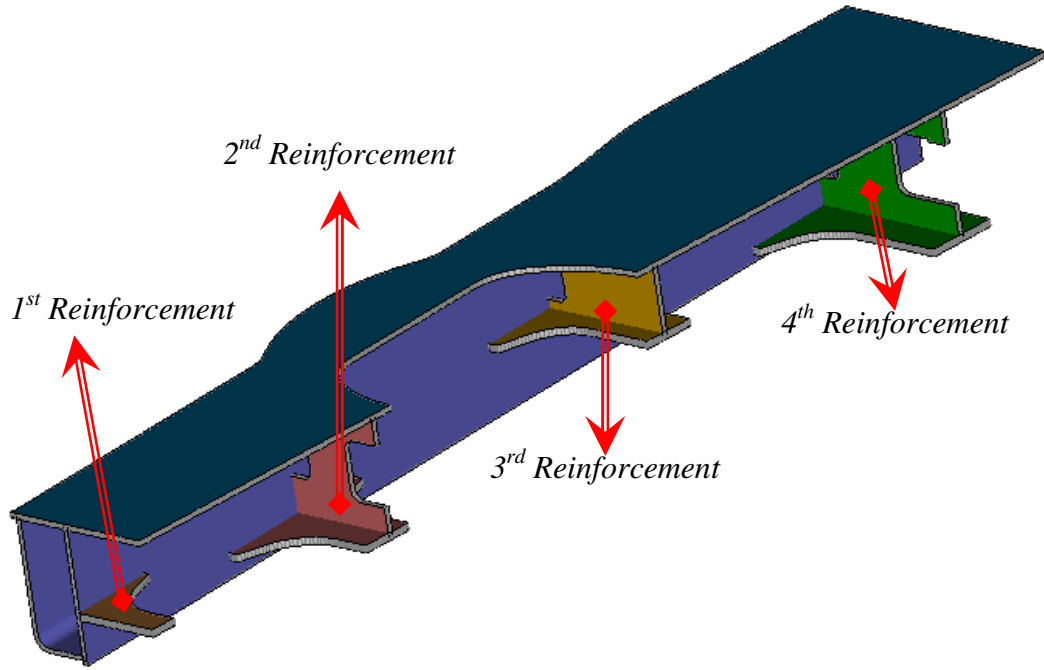
Figure 4.3 - The reinforcements between the side sections

The first reinforcement is welded parallel to the upper plate with a distance which is represented as b_1 in Figure 4.4. Similarly, horizontal plates of other reinforcements are placed parallel to the upper plate. The distances between the upper plate and the second, third and fourth reinforcements are represented as c_1, d_1 and e_1, respectively. The first reinforcement is placed in front of the middle part of the lower chassis. However, the location of other reinforcements can be changed with respect to the longitudinal axis of the excavator. The distances of the vertical plates of the reinforcements with respect to the rotation center of the upper chassis are shown as L_1, L_2 and L_3 in Figure 4.4. The width parameters of the horizontal plates of the reinforcements are defined by b_2, c_2, c_3, d_2, d_3, e_2 and e_3.
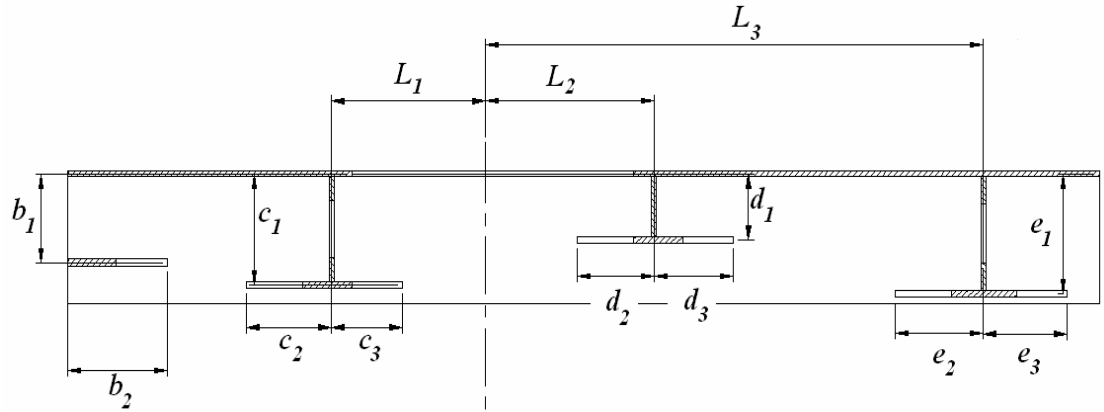
Figure 4.4 - The parameters of the reinforcements

4.2   Thickness Parameters of the Plates

The thickness parameters of the plates which are used in the lower chassis are very important for the strength analysis of the structure. So that, the thickness parameter of each plate is taken as variable within the optimization process. The thickness variables of the bended and the flat side plates and the upper plate are defined as t_1, t_2 and t_3, respectively.   The thicknesses of the horizontal plates of the reinforcements are shown as t_4, t_6, t_8 and t_{10} in Figure 4.5.

There are three stiffener plates located in the box section of the side plates. The location of the stiffeners is dependent with the other varying parameters. However, their thicknesses are variables which are defined as t_{f1}, t_{f2} and t_{f3}. The thickness variables of the vertical plates of the reinforcements are represented as t_5, t_7 and t_9 in Figure 4.5.
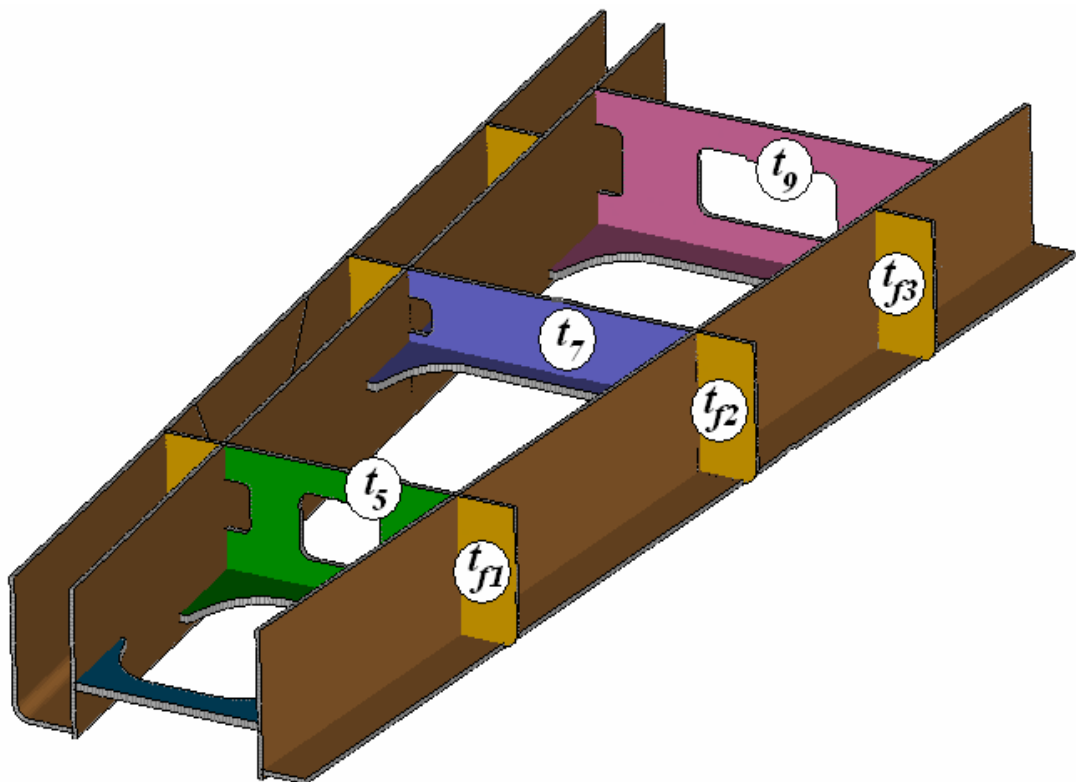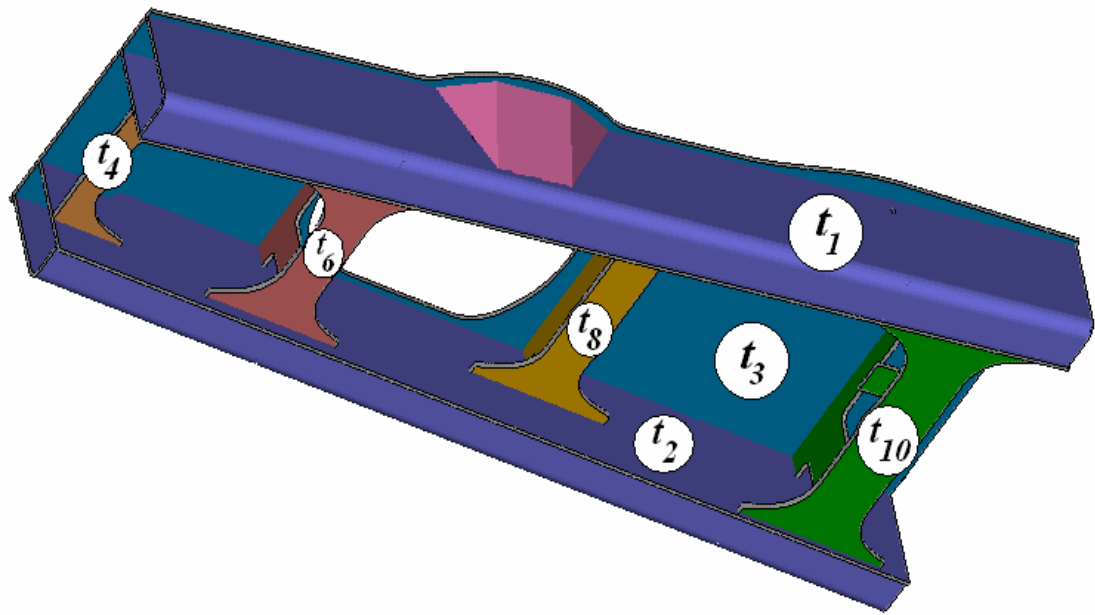
Figure 4.5 - The thickness variables of the plates

4.3 Generation of the Parametric Finite Element Model

A computer program has been developed to construct the geometry of the lower chassis with varying parameters. There are 18 geometrical parameters which define the shape of the model. More than 300 reference points are defined to form the geometry of the model. Then, the specified curves are generated to form the mesh of the model by using the reference points which are dependent on the defined geometrical parameters. The curves which are generated in the commercial pre-processor FEA program, MSC. Mentat, are shown in Figure 4.6.
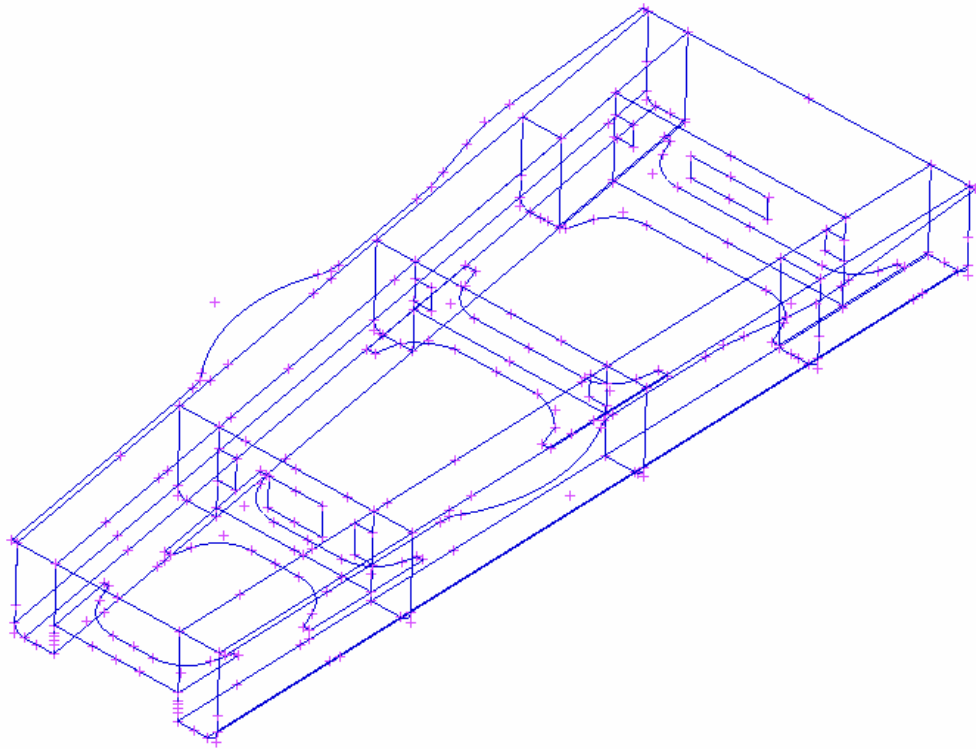
Figure 4.6 - Specified curves which are generated by using referance points

Planar shell elements are generated automatically by using the curves which are divided to generate the mesh with an appropriate element size. Finally, the mesh of the middle part of the lower chassis is assembled with the part which is generated by

the fixed parameters and the FEA of the structure is performed within the specified boundary conditions which are discussed in chapter 3 (Figure 4.7).
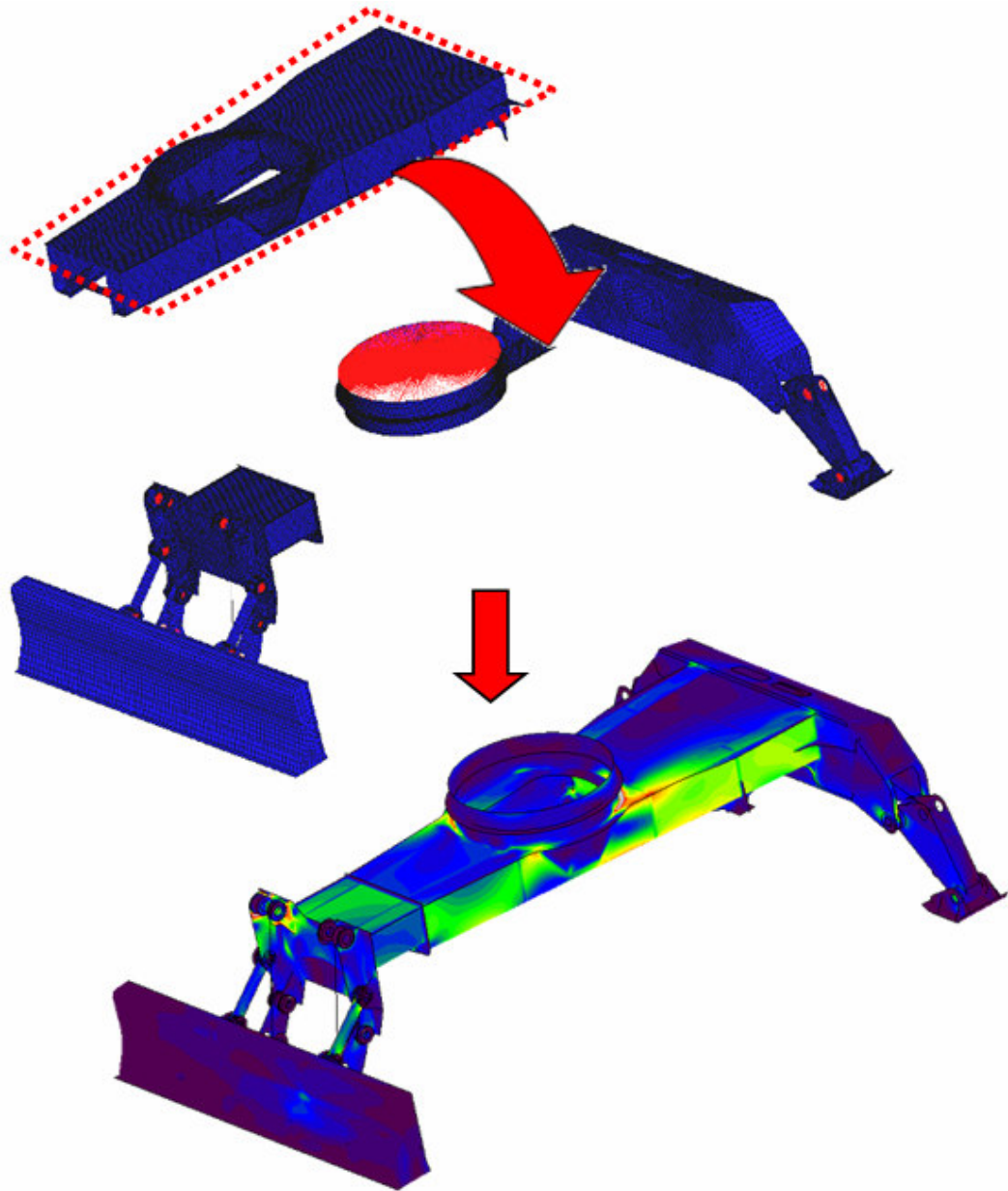
Figure 4.7 – Parametric modelling and FEA of the lower chassis

CHAPTER 5

DESIGN SPECIFICATIONS OF THE LOWER CHASSIS

Lower chassis is one of the main parts of the wheeled excavator and it is expected to operate without any failure during the whole life of the excavator. The lower chassis is manufactured by welding sheet metals each other, and the life of the welded steel structure is limited by the fatigue strength of the welded regions in the structure. Therefore, the welded regions of the lower chassis are investigated in this study. The welded regions of the structure are shown in Figure 5.1.
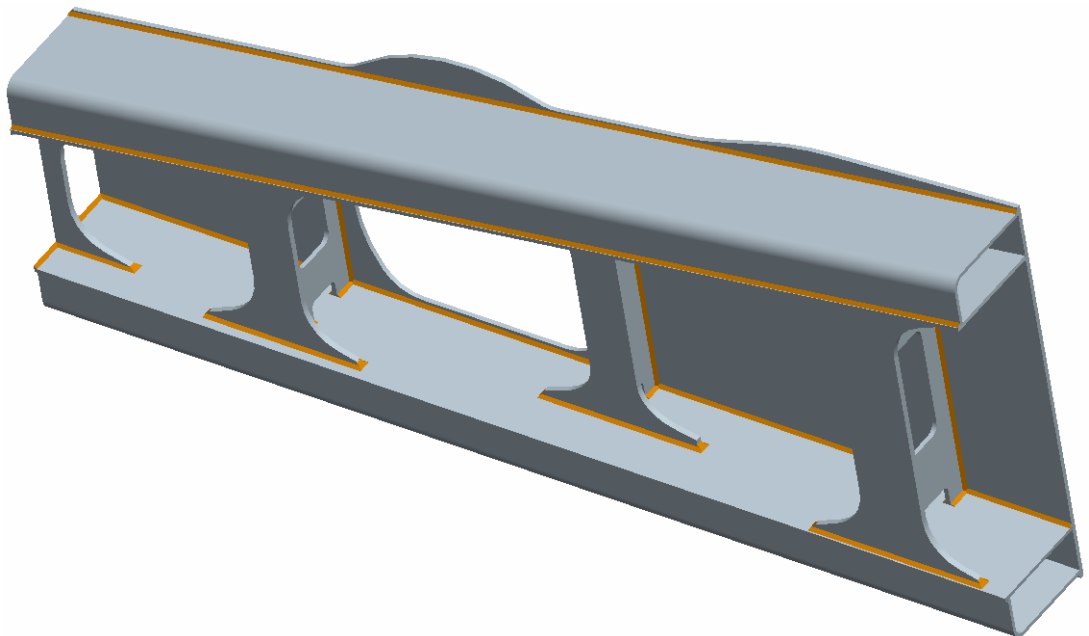
Figure 5.1- Welded regions in the structure

5.1   Stress Limitations of Welded Regions

The FEA model of the lower chassis is generated by using shell elements which are used to simulate sheet metals. The welding material is not defined in the models, so that the results of the connection lines of the sheet metals are not considered to estimate the fatigue life of the structure. Therefore, the stress value around the welded region is assumed as the nominal stress of the region.

In the literature, there are few documents about the fatigue life and nominal stress limitations of specified weld types and loading cases. In this study, the document of "Fatigue Design of Welded Joints and Components" [7] which is published by The International Institute of Welding (IIW) is used to determine the stress limitations for the welded regions. Different types of welding and loading cases exist in the document. These cases are classified according to their fatigue strength characteristics. Fatigue resistance S-N curves of the classified weld types are shown in Figure 5.2. Each curve is identified by the stress limitation at 2 million cycles. This value is named as the fatigue class (FAT) of the welding types in the specified loading conditions.

Each type of welding and loading case in the lower chassis is matched with the corresponding condition which is stated in the document. Then, the stress limitations are evaluated for the welded regions in the structure. The conditions which are stated in the document are defined for simple structures and uniaxial load cases. So that, they may not simulate the specified regions exactly, since the lower chassis is a complex welded structure. Therefore, some of the stress limitation values which are evaluated by using the S-N curves in the document are modified with the experience based on the fatigue tests and FEA of welded structures, cracks and failures which occurred in the previously manufactured structures.

47
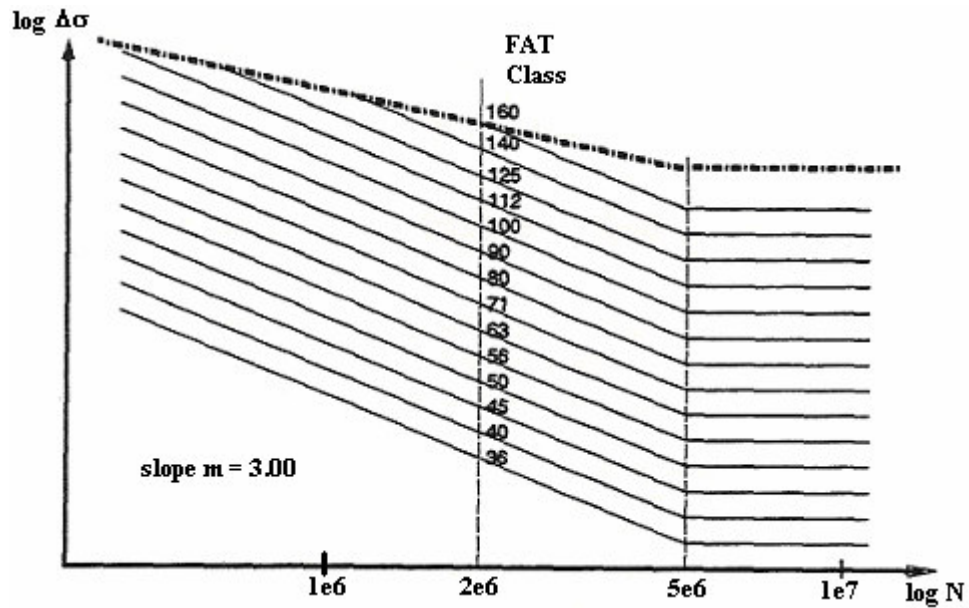
Figure 5.2 - Fatigue resistance S-N curves for steel [7]

Fillet weld is generally used for the production of the middle part of the lower chassis. The sheet metals which are perpendicular to each other are joined with fillet welds. The loading cases in the welded regions of the structure are separated to three main types.

In the first type, the loading direction is perpendicular to the fillet weld, the second type simulates the condition where the loading direction is parallel to the fillet weld and the stress limitations for the ends of the reinforcements on the side plates are discussed in the third type.

5.1.1   Type 1: Loading Direction is Perpendicular to Fillet Weld

The condition which is numbered by 511 in the document of IIW is the most suitable one for the welded regions where loading direction is perpendicular in the structure

(Figure 5.3). The perpendicularly oriented plates do not carry any load and the plates are thicker than the loaded plates. So that S-N curve of FAT class 71 is used to evaluate the stress limitations for the type 1 welded regions.
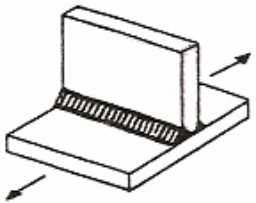
No.	Structural Detail (Structural Steel)	Description	FAT
511		Transverse non-load-carrying attachment, not thicker than main plate	
		K-butt weld, toe ground	100
		Two-sided fillets, toe ground	100
		Fillet weld(s), as welded	80
		Thicker than main plate	71

Figure 5.3 – Fatigue resistance of specified weld type for perpendicular loading [7]

The region under the third reinforcement on the side plate is one of the type 1 welded regions in the structure. The direction of maximum principle stress under the third reinforcement is represented in Figure 5.4.
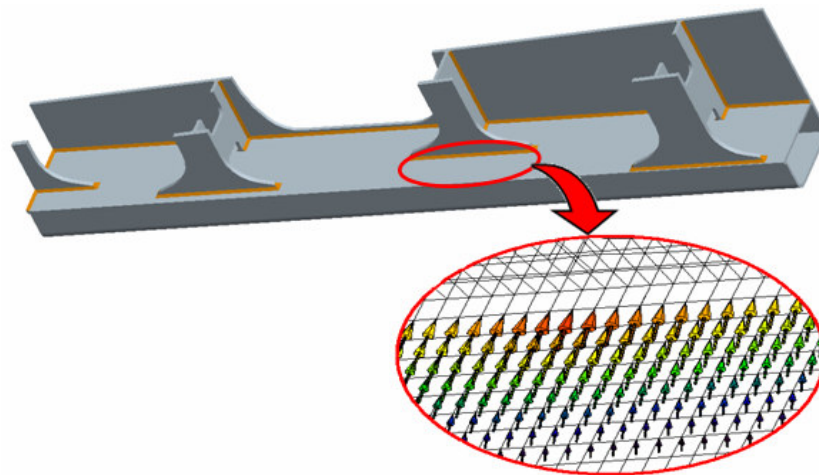
Figure 5.4 - Maximum principal stress direction around the welded region

5.1.2   Type 2: Loading Direction is Parallel to Fillet Weld

The welded regions where loading direction is on the longitudinal axis of the fillet weld are matched with the condition which is numbered by 323 in the document of IIW (Figure 5.5). All parts of the lower chassis are welded manually. S-N curve of FAT class 90 is used to evaluate the stress limitations for the type 2 welded regions.
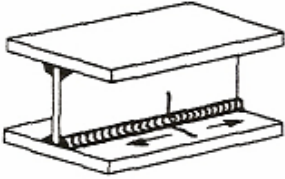
No.	Structural Detail (Structural Steel)	Description	FAT
323		Continuous manual longitudinal fillet or butt weld (based on stress range in flange)	90

Figure 5.5 - Fatigue resistance of specified weld type for longitudinal loading [7]

The direction of maximum principle stress under the side plates is parallel to the fillet weld that connects the side plates (Figure 5.6). Therefore, the welded region under the side plates is considered as the type 2 welded region.

5.1.3   Type 3: Stress Concentration at Weld Ends

The reinforcements of the structure are welded to the side plates and stress concentration may occur at the end of fillet welds of the reinforcements (Figure 5.7).

This situation is similar to the condition which is numbered by 512 in the document of IIW (Figure 5.8). The plates of the reinforcements are thicker than the side plates. According to this, S-N curve of FAT class 71 is used for the type 3 weld regions.

Figure 5.6 - Maximum principal stress direction around the welded region
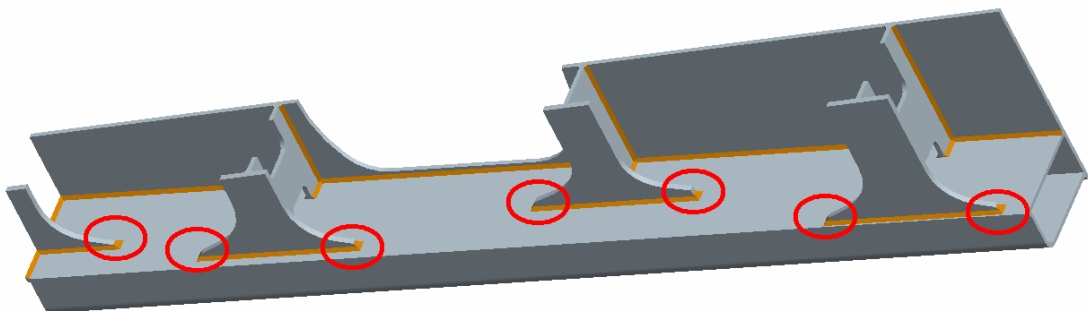
Figure 5.7 - Weld ends of the reinforcements

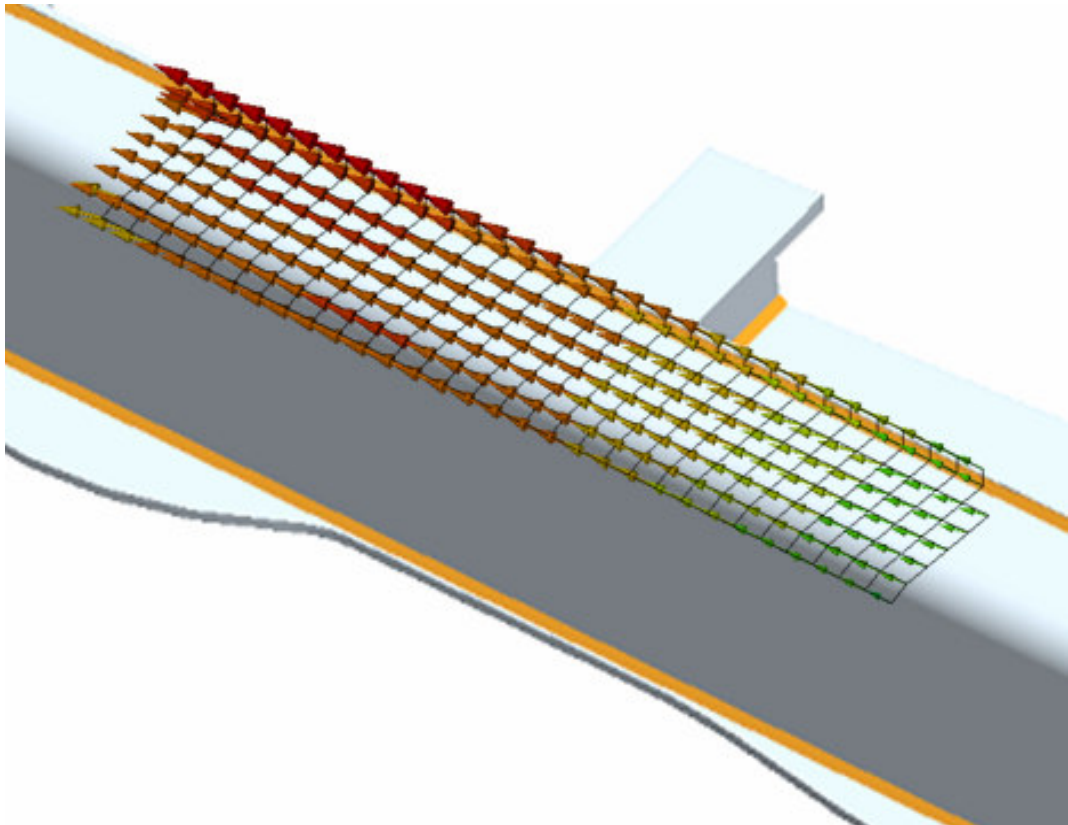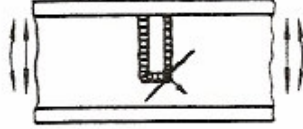| No.	Structural Detail (Structural Steel)	Description	FAT
512		Transverse stiffener welded on girder web or flange, not thikker than main plate. For weld ends on web principle stress to be used	
		K-butt weld, toe ground	100
		Two-sided fillets, toe ground	100
		Fillet weld(s): as welded	80
		thicker than main plate	71

Figure 5.8 - Fatigue resistance of reinforcement weld ends [7]

5.2   Weight Limitation

The lower chassis is tried to be manufactured with lightweight sheets due to material cost. This fact should be considered while satisfying required fatigue strength. On the other hand, wheeled excavators may be driven over long distances on road and the weight of the structure affects the fuel consumption.

5.3   Other Design Limitations

As it is mentioned before, the hydraulic motor and the transmission are placed under lower chassis. To accommodate these parts, there must be adequate space between the second and the third reinforcements. Moreover, the parts of the lower chassis are welded manually and welding operation must be considered especially for the determination of the parameters of the reinforcements.

Rear axle of the wheeled excavator is connected to the parts which are located on the lower chassis. The distance between these parts are represented as d_{ra} in Figure 5.9. Although it is possible to modify the connection parts of the lower chassis, d_{ra} may vary in a limited range.
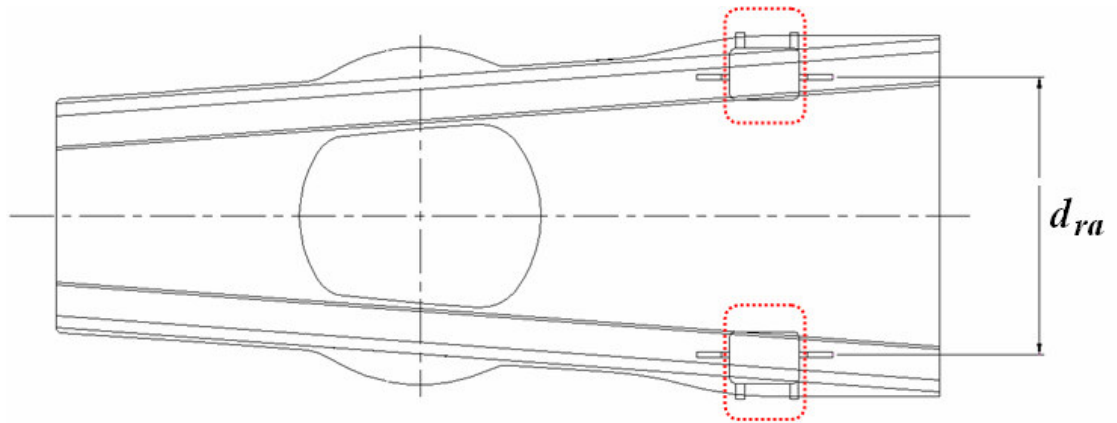
Figure 5.9 - Connection parts of rear axle

CHAPTER 6

OPTIMIZATION OF THE DESIGN

The optimization algorithm of the lower chassis is basically a modification of the algorithm used by Uzer [5]. The flowchart and basic parameters of the algorithm have been rearranged and transformed to an appropriate form suitable for the lower chassis design.

Optimization process of the lower chassis intends to minimize the mass while the structure satisfies the required fatigue resistance. Hence, the design problem of this study is a minimization problem with specified constraints. There are 31 design variables that define the geometry of the lower chassis. Objective function of the problem is dependent on the design variables. Genetic algorithm is used to solve the optimization problem. In this chapter, the optimization of the design will be discussed in detail.

6.1   Design Variables

As it is mentioned before, several parameters are required to form the geometry of the lower chassis. Some of the parameters are fixed in order to reduce optimization process time. 31 parameters that affect the design specifications significantly are selected as variables. The selected design variables are discussed in chapter 4.

Design variables may change within a range which is specially defined for each variable. Ranges of the variables are set meticulously by considering the manufacturing process of the structure. Moreover, the ranges are restricted not to generate unfeasible models by engineering inspection.

The sensitivity and the precision of the variables are important issue that must be considered. It is meaningless to generate the geometry with too sensitive variables if the accuracy of the FEA results is not equally sensitive. Moreover, it is not possible to manufacture welded structures with highly precise dimensions, since tolerance ranges of welding process is limited. According to these, the sensitivity of length variables is taken as 1 mm and it is set to 10^{-4} radians for the angle variable (α) of the design. On the other hand, thickness variables are restricted with the product range of the sheet metal suppliers. Available sheet metal thicknesses that can be used in the design are 6, 8, 10, 12, 15, 18, 20, 22, 25 and 30 mm.

6.2   Objective Function

The aim of the optimization is to minimize the mass of the lower chassis. Hence the objective function of the minimization problem is mass of the structure. Objective function is denoted as;

$$O(X)=M(X)$$

The set of design variables is defined as X. M(X) designates the mass function of the structure. All parts of the structure are produced by using same type of steel. Therefore, density of the material is not a variable of the mass function that depends on only the set of design variables.

The minimization problem includes the constraints that are discussed as stress limitations in chapter 5. Maximum stress at each welded region must be lower than the corresponding critical value. Stress limitations for the specified welded regions are represented as;

$$\sigma_i^{\max}(X) \leq \sigma_i^{\lim} \qquad i = 1, 2, ..., n$$

$\sigma_i^{\max}(X)$ is the maximum stress at the ith welded region of the structure, and $\sigma_i^{\lim}$ is the limit stress value for the ith welded region. The number of the specified regions is denoted as n.

In this study, the number of the constraint equations based on the stress limitations is very high, and it is very difficult to find feasible solutions in highly constrained problems. To eliminate these constraints, the maximum stress values which are higher than the limit stress values are considered in the evaluation of the objective function. The square of the difference between the maximum and the limit stress is multiplied by predetermined coefficients for each welded regions and added to the objective function. The square of the difference between the maximum and the limit stress is represented as $p_i(X)$. The modified objective function is called as penalty function of the optimization problem and denoted as $P(X)$ below;

$$p_i(X) = \begin{cases} \sigma_i^{\max}(X) - \sigma_i^{\lim}, & \sigma_i^{\max}(X) > \sigma_i^{\lim} \\ 0, & \sigma_i^{\max}(X) \leq \sigma_i^{\lim} \end{cases}$$

$$P(X) = O(X) + \sum_{i=1}^{n} r_i [p_i(X)]^2$$

where

r_i is the penalty coefficient of ith region.

The penalty coefficients and the power of $p_i(X)$ function are important for results of the optimization process. They may change with respect to characteristics of problem and they should be assigned to suitable values to achieve feasible results.

Finally, the penalty function is formed and minimized during the optimization process. Hence, the constrained minimization problem is converted to the unconstrained minimization problem.

6.3   Solution of the Optimization Problem

Genetic algorithm (GA) is utilized to solve the defined optimization problem. First of all, it is easy to implement GA into shape optimization problems. GA generates new population according to fitness values of previous population by using special operators and does not require any information about evaluation of fitness values. In this study, the evaluation of the fitness values depends on the FEA of the structure and it is totally independent from the GA part of the program. Secondly, GA is an effective tool for shape optimization problems. It is shown that GA leads to good results for the structural optimization in the thesis of Uzer[5].

The flow diagram of the program is shown step by step in Figure 6.1. The model manager which generates the FEA models with respect to varying design variables is embedded into the Excel file including GA macro codes. The FEA of existing population and the result files are generated by the model manager. Required data is taken from the result files to evaluate the fitness value that is inversely proportional to the penalty function in this study. The GA operators used in this study are

elimination, parent selection, crossover and mutation. New population is generated by applying these operators. Each stage shown in Figure 6.1 is discussed in detail.
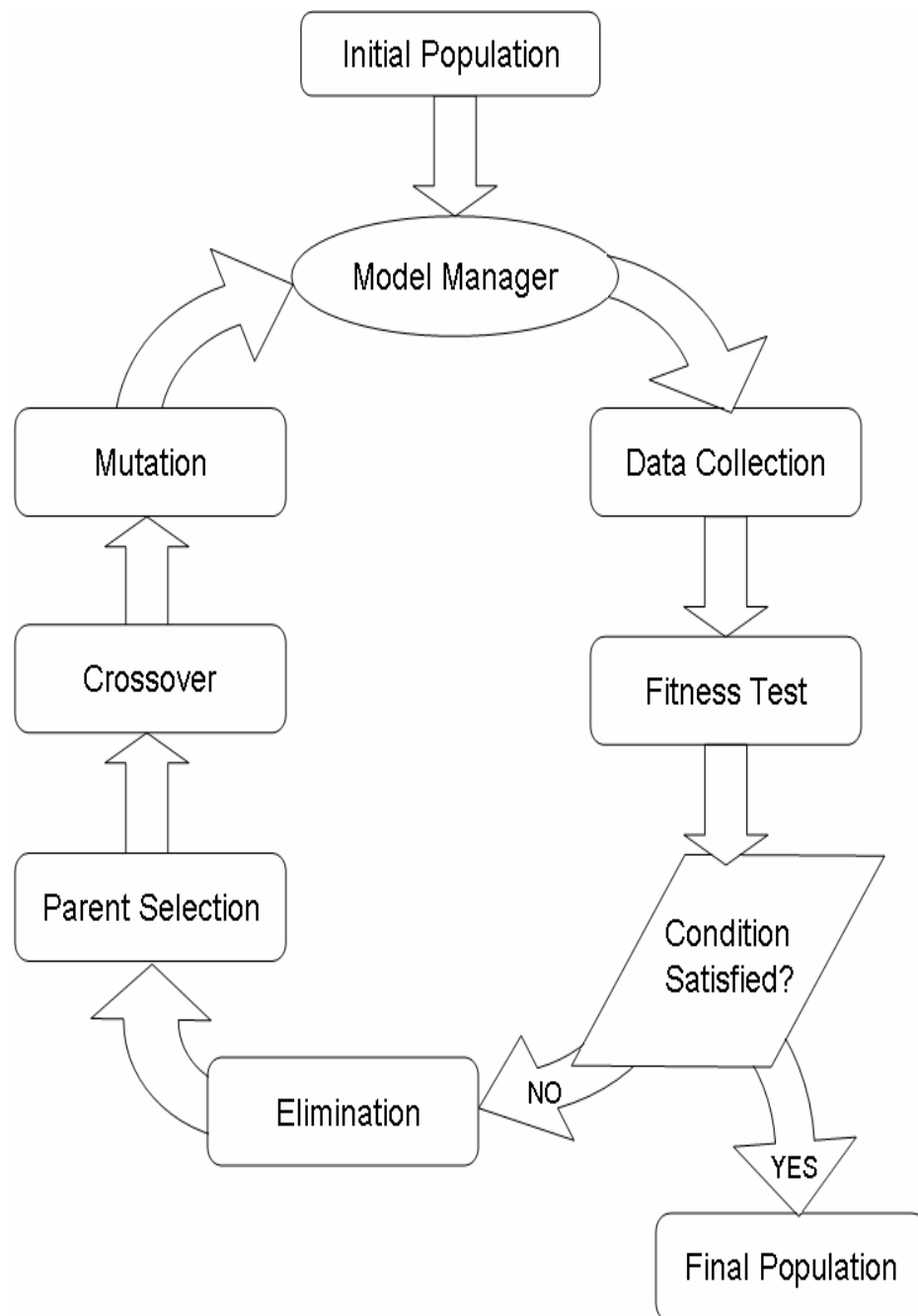

Figure 6.1 - Flow diagram of the program

6.3.1   Initial Population

Firstly, solution sets are usually generated by selecting the design parameters randomly to generate the initial population. In such cases, initial population may include some solution sets which are generated by engineering intuition. In this study, a solution set is generated by existing design parameters and the other solution sets are created randomly.

The population size of GA is an important parameter for the process time of the optimization algorithm. GA may give good results within few generations when population are generated with high number of individuals, but process time of the program increases directly proportional to the number of individuals in population. Appropriate size of populations may differ for different types of optimization problems In this study, the number of the initial population individuals is equalized to the number of individuals in the general population and it is taken as 20 for all case studies.

6.3.2   Model Manager

Model manager performs the FEA of the individuals of lastly generated population. Individuals of population have 31 chromosomes. This means that solution sets of the problems include 31 design parameters. Firstly, the coordinates of the reference points are evaluated in the Excel platform. Then, the FEA model is generated in the commercial program, MSC. Marc Mentat. After the generation of model, mass of the structure is found by using the mass evaluation feature of the pre-processor of the FEA program.

Secondly, the FEA is performed within same boundary conditions for each individual. Results files of the FEA program are generated in a specific data storage format (.t16) which includes all displacement, strain and stress data of the FEA.

6.3.3 Data Collection

Stress data of the structure is collected from the results files of MSC Marc. A computer code that is based on Python is used to take the results in the determined regions. The regions are shown in Figure 6.2. The locations of the regions may differ for different models. So that the specified coordinates of the determined regions are recorded in a text file after the model manager generates the reference points of the FEA. Python based computer program collects stress data from the determined regions which are positioned with respect to the coordinates written in the text file.
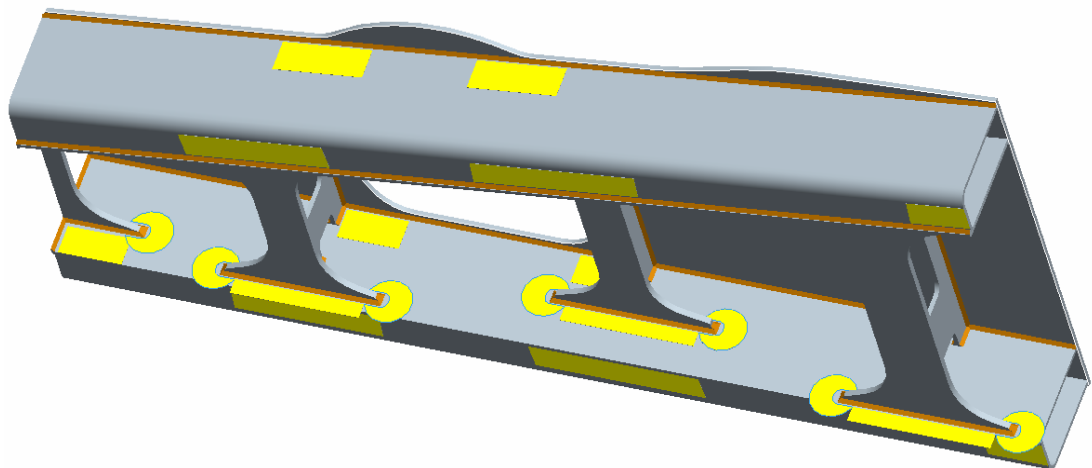

Figure 6.2 - Stress data is collected from the determined regions

6.3.4 Fitness Test

Since this study is based on a minimization problem, it is aimed to minimize the modified objective function which is previously mentioned as penalty function. Fitness function is defined to specify strength of the individuals in population. Fitness function is inversely proportional to the penalty function.

$$F(X) = \frac{m^{target}}{P(X)} \times 100$$

where

$F(X)$ is the fitness function

$P(X)$ is the penalty function

m^{target} is the target mass of the structure

6.3.5 Termination Condition

In general, termination criteria of optimization programs are based on the number of iterations or the target of objective function. Also, non-commercial optimization programs are usually stopped by users to achieve optimum result within maximum available process time. In this study, the program terminates the loop and creates the final population when the fitness function of an individual in population reaches 100. This means that target mass of the structure is achieved while satisfying all stress and other constraints. However, the program is stopped if the generation number is 100, although the termination criterion is not satisfied.

6.3.6   Elimination

First processor of GA used in the program is elimination. If the termination criterion is not satisfied, then the individuals with fitness values lower than the average fitness value of the population are eliminated. In some cases, the population has similar individuals and the fitness values of the individuals are almost equal. This causes killing high or low number of individuals of the population, since the fitness values of the individuals is close to the average fitness value of the population. This is not a desired situation, because variation is important to find an optimum individual. To overcome this problem, all members of the population are generated randomly again if the ratio of killed or alive individuals to the whole population is smaller than 5%.

6.3.7   Parent Selection

It is required to generate new individuals with the same number of eliminated members. New individuals are produced by coupling the selected parents. In this study, half of the parents are selected from the individuals with higher fitness values. The rest of the parents are selected randomly from the whole population to provide variety in the population. Therefore, an individual can be selected as a parent twice. If same individuals are coupled, same individuals are produced as children. Hence, coupling of same individuals are prevented in the program.

6.3.8   Crossover

Two individuals are generated with crossover operation by each selected couple. At the beginning of the crossover operation, a random real number between 0 and 1 is

generated. Generated random number is called as r. Each genome of the generated individuals is found from the weighted mean of the genomes of the parents. To evaluate the weighted mean of the genomes, r is used for first child and $(1-r)$ is used for second child. r is not changed during a crossover operation.

6.3.9   Mutation

Mutation is an important operator of GA to perform variety of individuals in population. In this study, two randomly selected genomes of individuals are mutated. The individual with the best fitness value is never mutated to protect the best individual of the population.

CHAPTER 7

CASE STUDIES

In this chapter, results of four sample runs of the optimization program will be presented. The geometries of the results are compared with the existing design. Also, FEA results of four optimum solutions and the initial design are shown.

It is tried to reach optimum solution by changing 31 variables for the first and the second sample runs. However, the thickness parameters of the side plates and the upper plate, t_1, t_2 and t_3, are fixed with the initial design parameters for the third sample run. Fourth one is a special case where the third reinforcement is not used. It is aimed to find an optimum design which does not contain the third reinforcement in the fourth sample run.

Desired stress values for the welded regions of the structure and the penalty coefficients of the penalty function are same for all sample runs. The results of the second and the third cases are almost 1% lighter than the initial design. However, the first and the fourth sample runs resulted in 1% heavier models than the existing model. The geometries of the results are compared with the initial design in figures 7.1 to 7.4. Also, Von Mises stress distribution over the models of the results and the existing design is presented in figures 7.5 to 7.8.
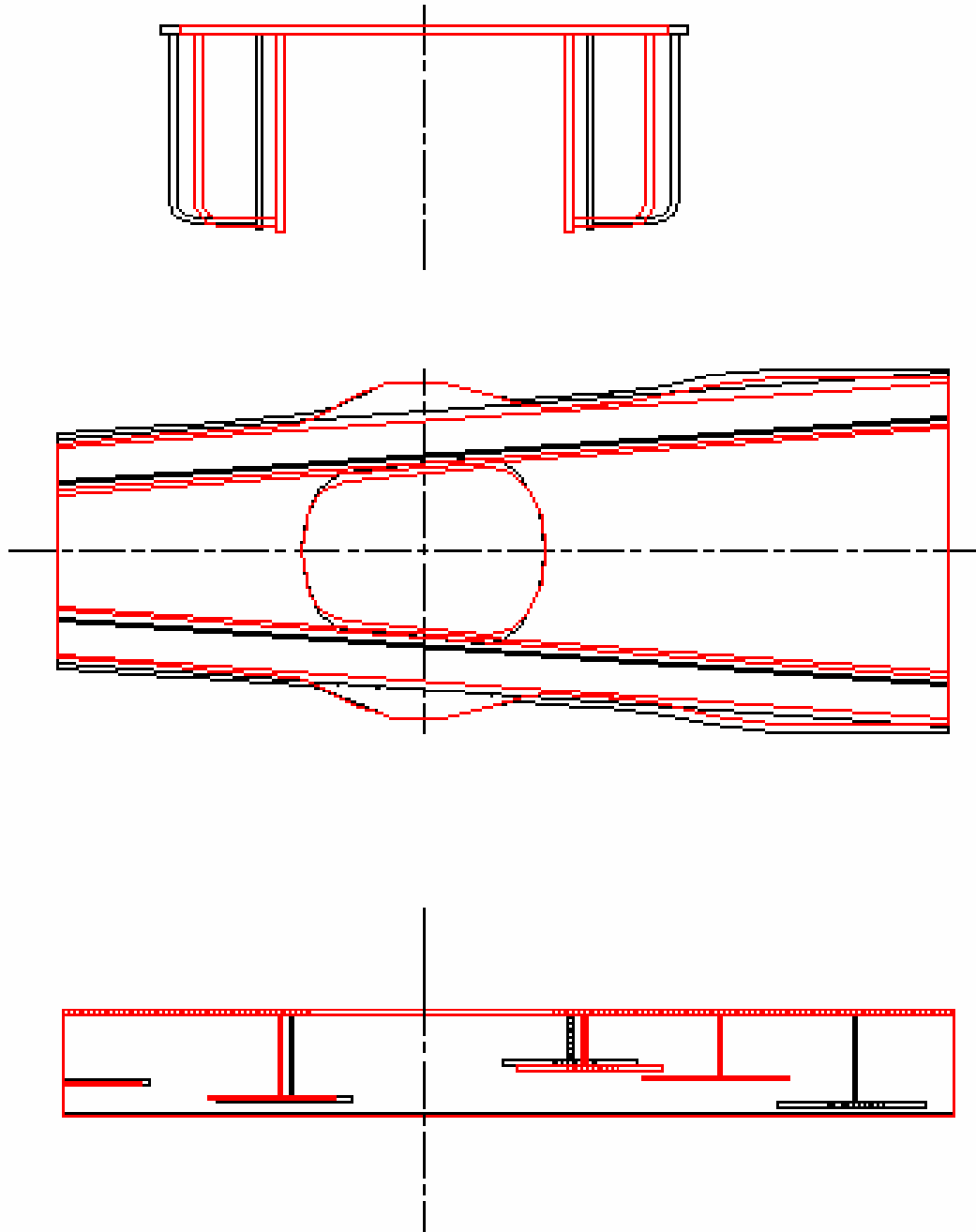
Figure 7.1 - Comparison of the initial design and the result of sample run #1
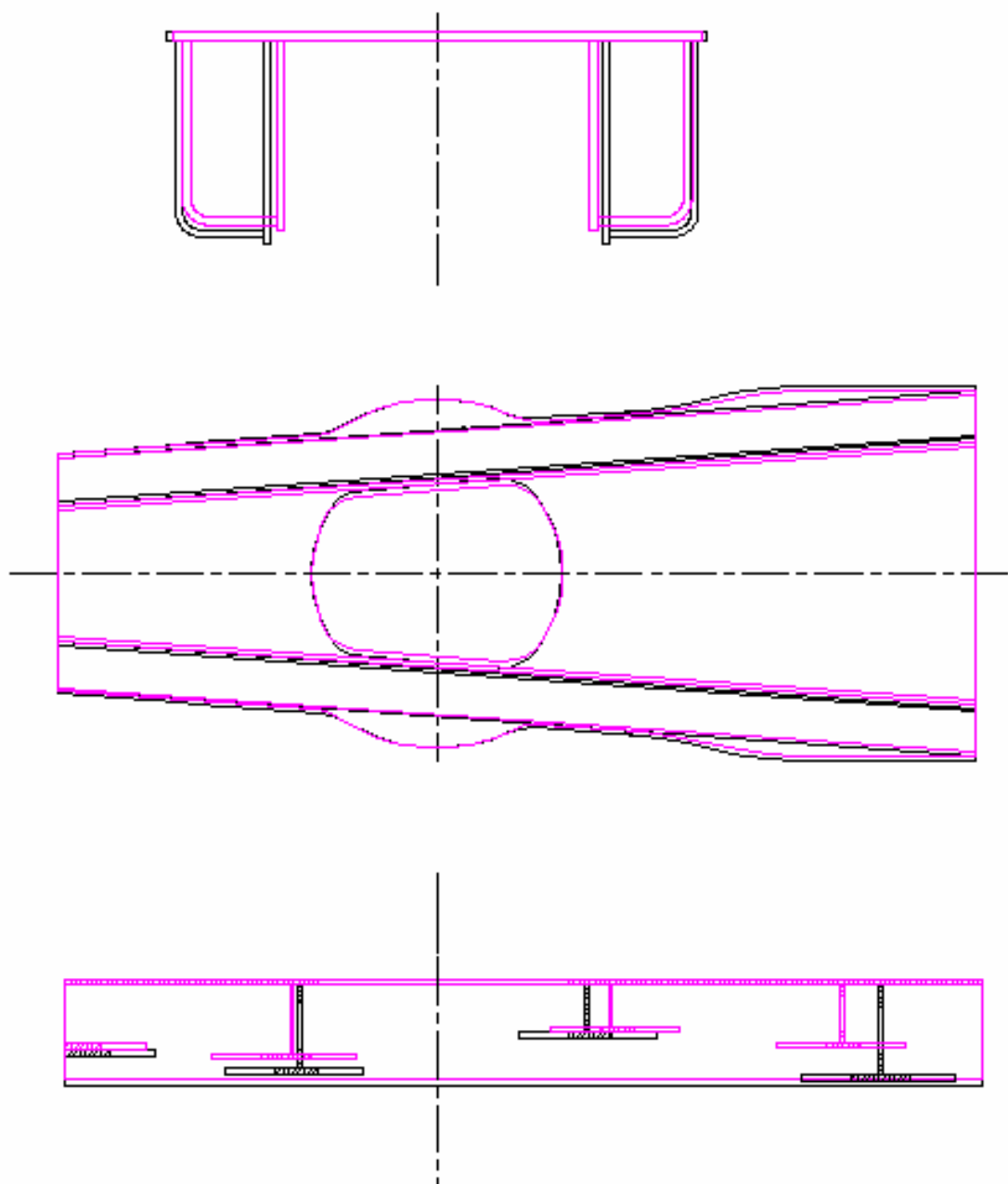
Initial Design

Result of Sample Run #2

Figure 7.2 - Comparison of the initial design and the result of sample run #2
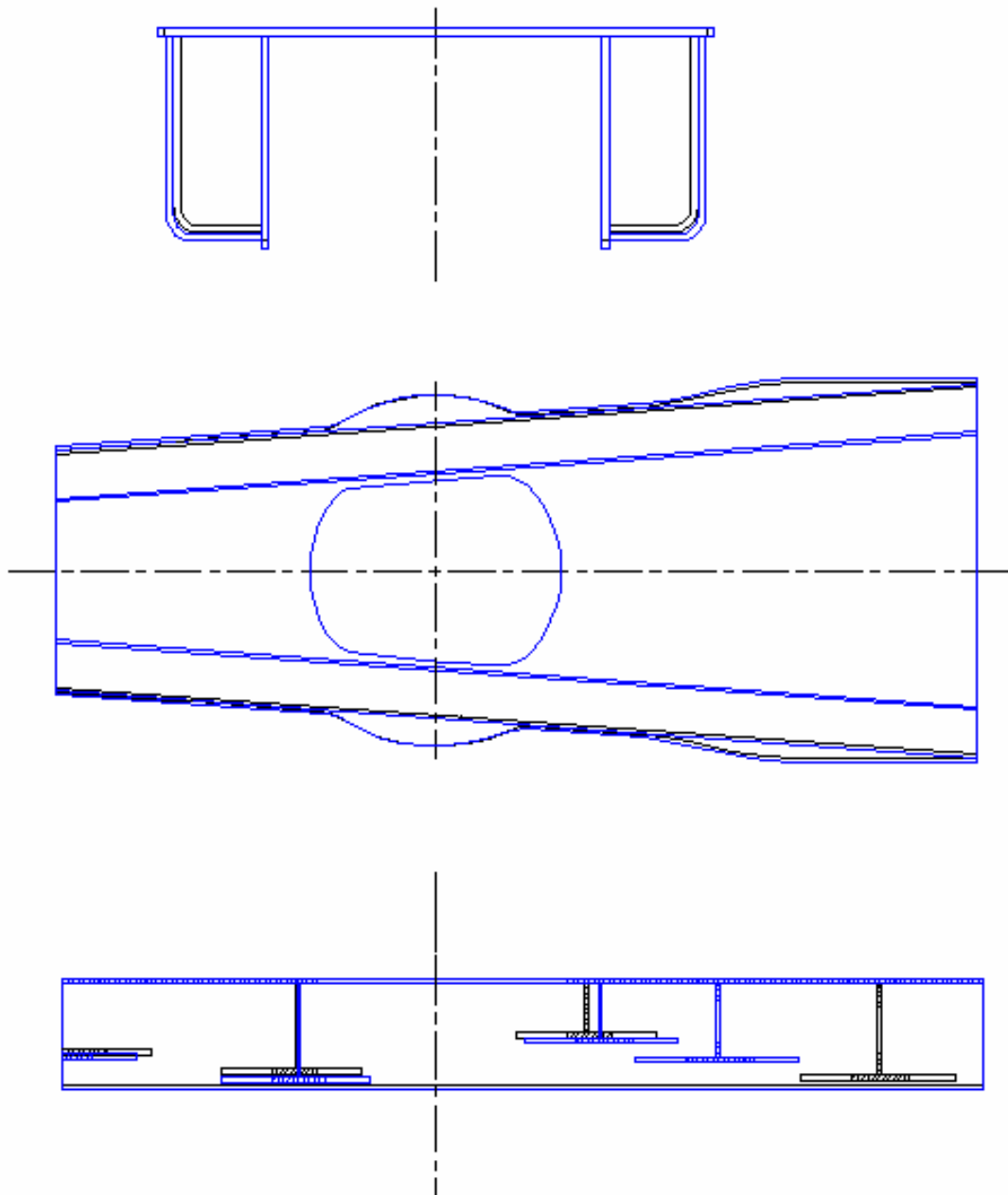
Initial Design

Result of Sample Run #3

Figure 7.3 - Comparison of the initial design and the result of sample run #3
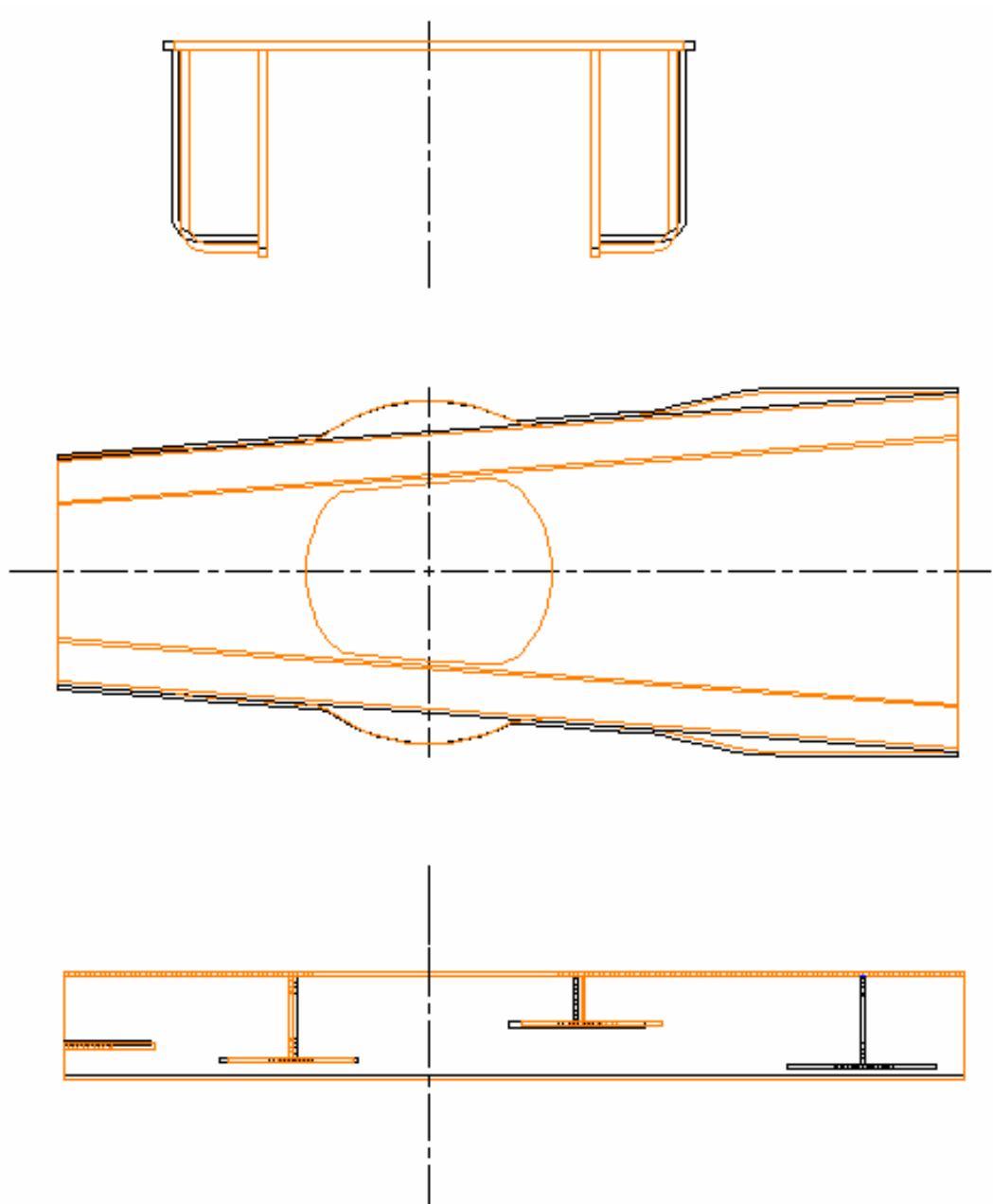
Initial Design

Result of Sample Run #4

Figure 7.4 - Comparison of the initial design and the result of sample run #4

Figure 7.5 - Left side view of models representing stress distributions at load case 1.
(a) Sample run #1. (b) Sample run #2. (c) Sample run #3. (d) Sample run #4.
(e) Initial design.

Figure 7.6 - Right side view of models representing stress distributions at load case 1.
(a) Sample run #1. (b) Sample run #2. (c) Sample run #3. (d) Sample run #4.
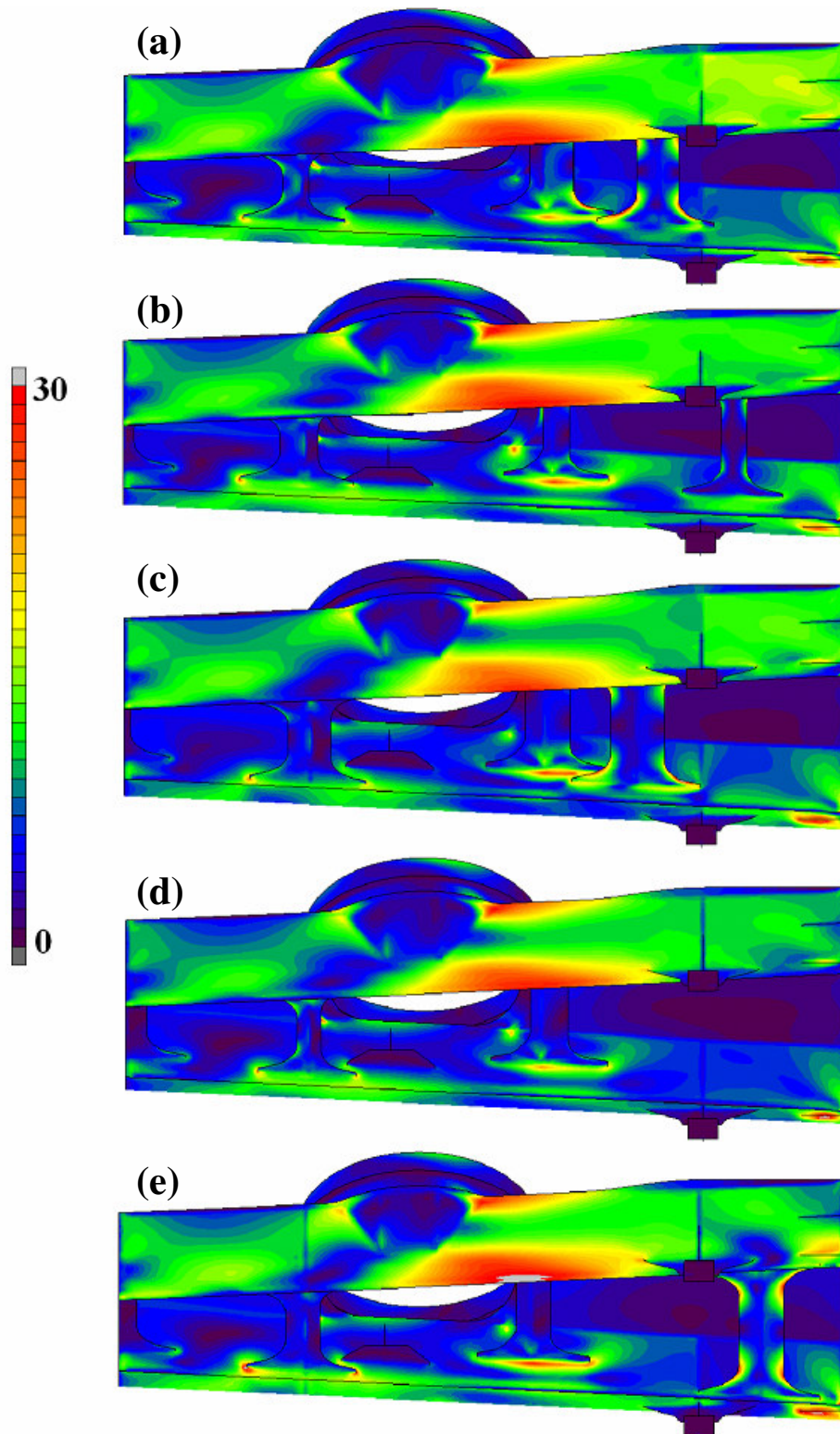(e) Initial design.

Figure 7.7 - Left side view of models representing stress distributions at load case 2.
(a) Sample run #1. (b) Sample run #2. (c) Sample run #3. (d) Sample run #4.
(e) Initial design.

Figure 7.8 - Right side view of models representing stress distributions at load case 2.
(a) Sample run #1. (b) Sample run #2. (c) Sample run #3. (d) Sample run #4.
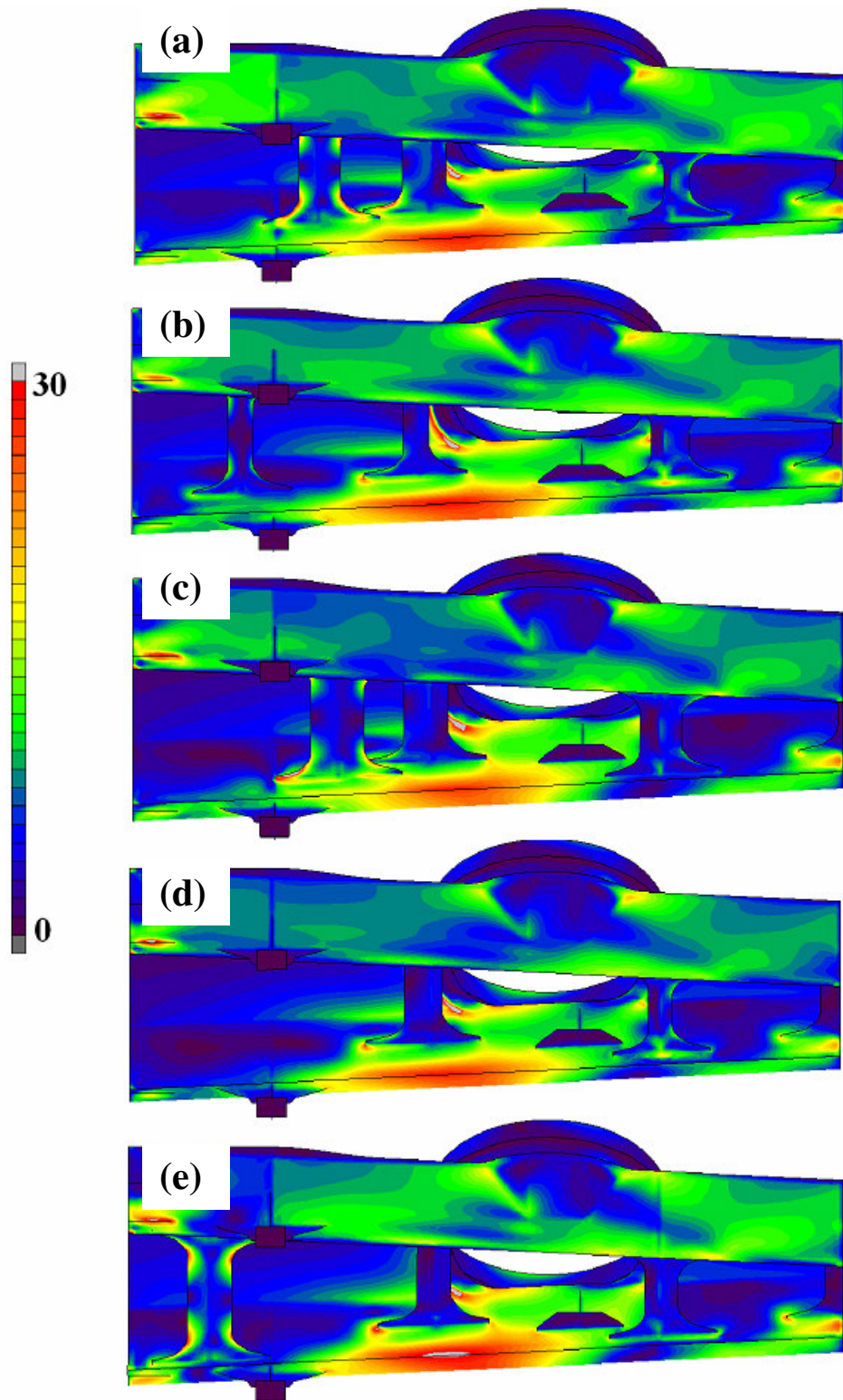(e) Initial design.
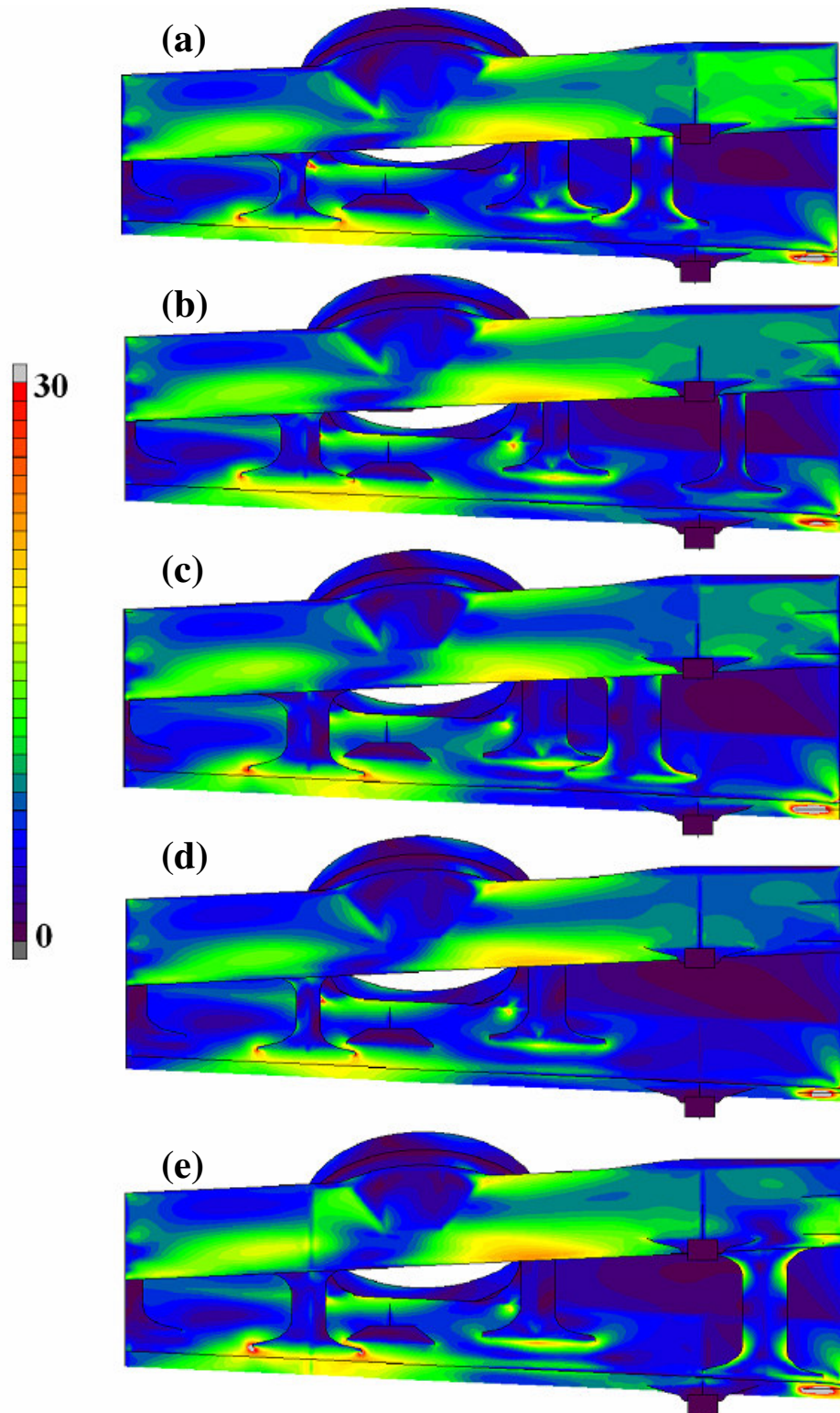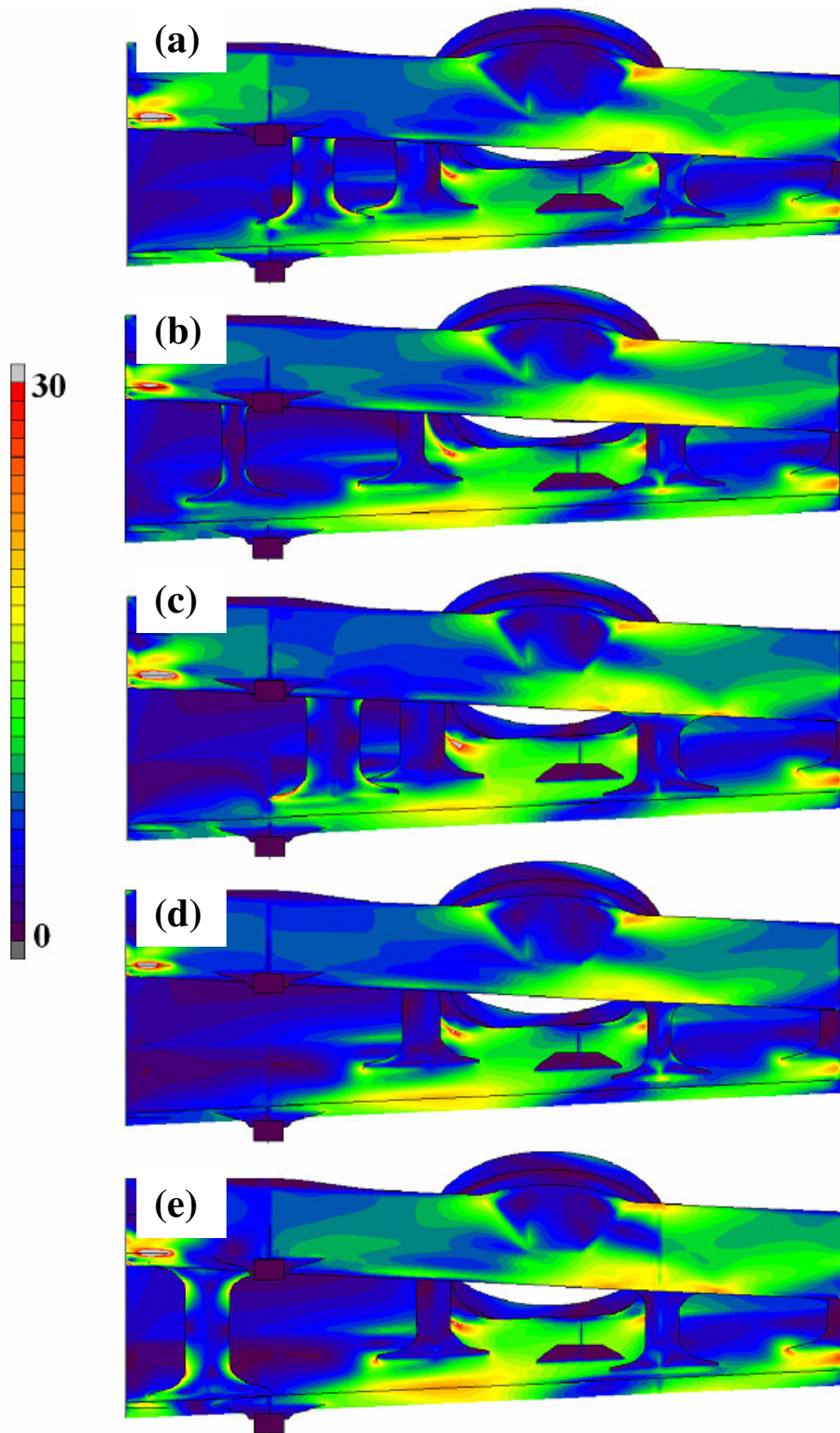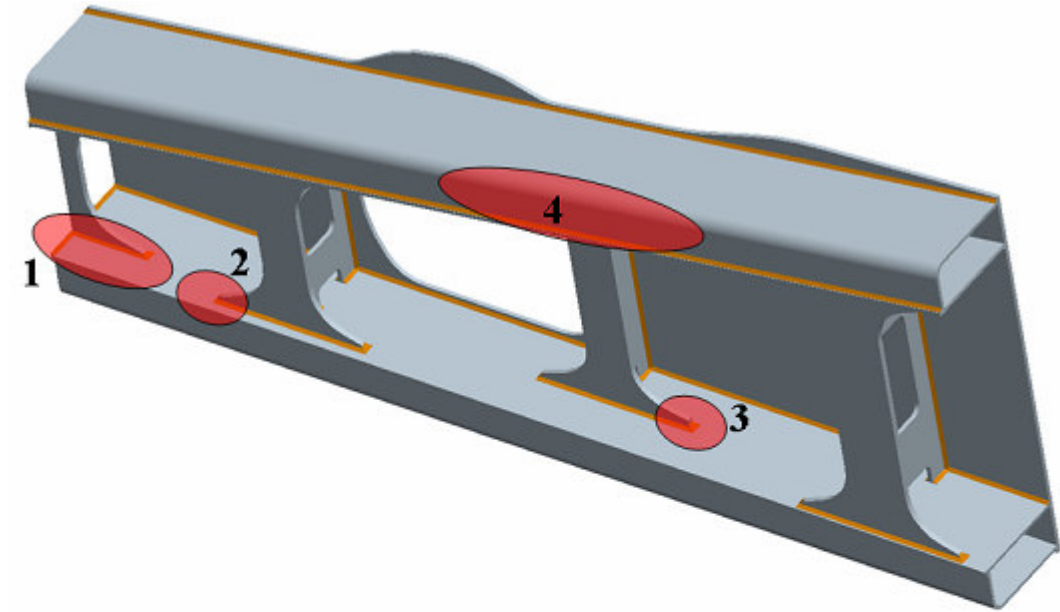
As can be seen, the solutions having higher strength properties are performed by using almost same amount of sheet metals. Furthermore, remarkable improvement is observed in the regions that fatigue failure occurred in the past (Figure 7.9). The ratio of the maximum Von Mises stress to the limit stress for those regions is presented in Figure 7.9.

Case / Region No.	Initial	Run#1	Run#2	Run#3	Run#4
1	1.09	0.96	0.92	1.05	0.91
2	1.37	0.91	0.88	1.01	0.90
3	1.12	0.91	0.99	1.01	0.86
4	1.11	1.02	1.02	0.96	1.01

Figure 7.9 - The critical welded regions and the ratio of the maximum stress to the limit stress for those regions

All of the samples are started with different random initial parameter values except one individual which contains the parameters of the existing design. For all runs of

the program population size is set to 20. The optimization program is run for 100 generations of population. A single generation of a population approximately takes 90 minutes in a computer with Intel Core 2 Duo 2.66 and 4 gb ram. So that, the program is run more than 6 days for each sample. The fitness evolution over the generations of the samples are presented in figures 7.10 to 7.13.
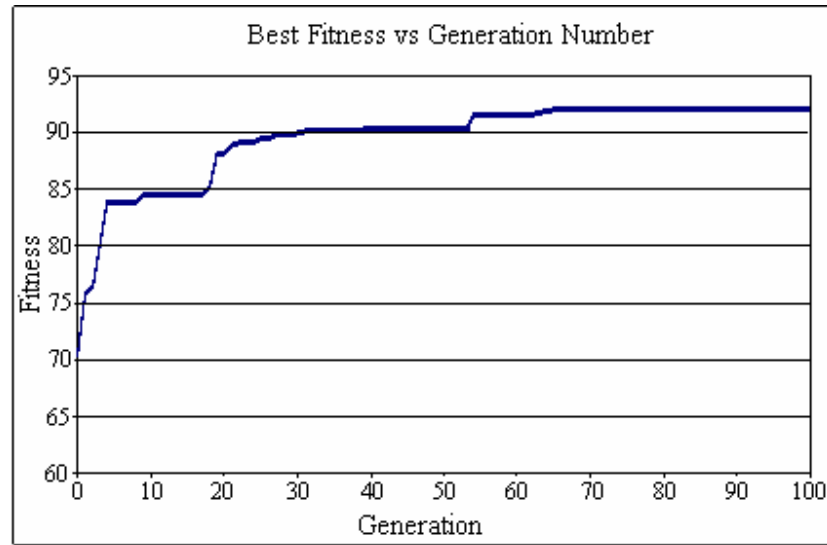

Figure 7.10 - Best fitness vs. generation number plot for sample run #1
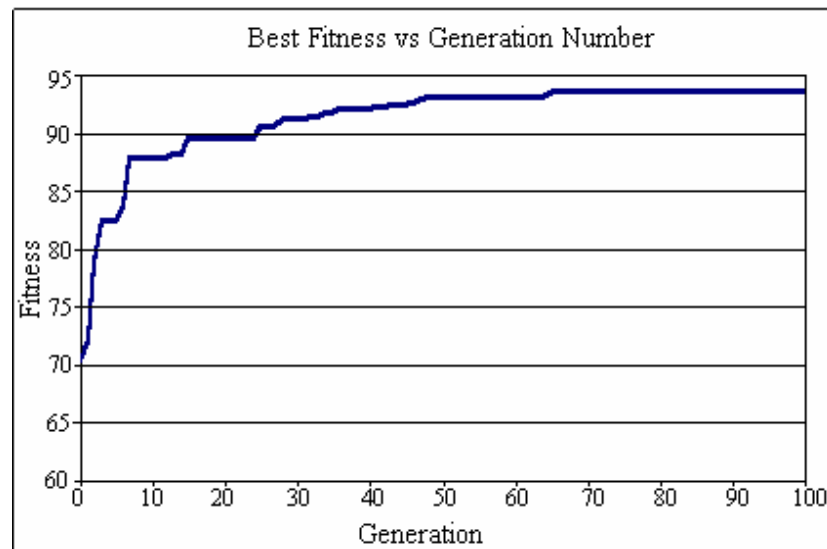

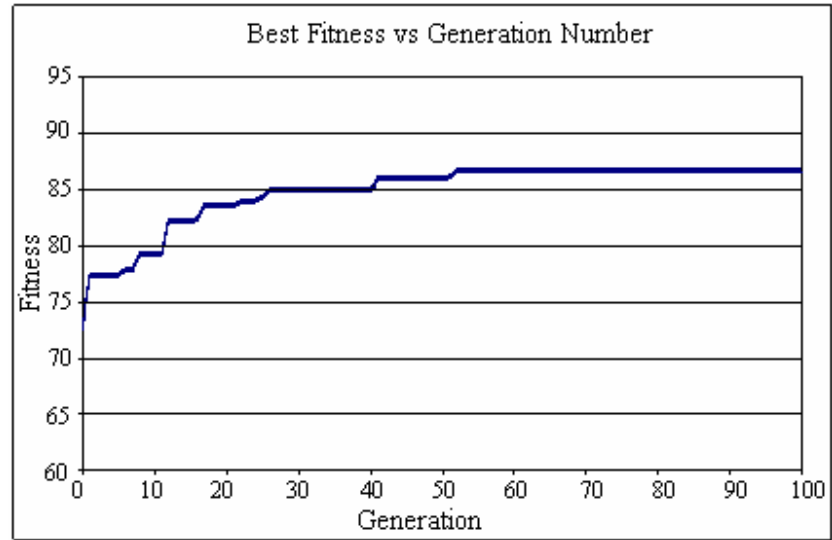Figure 7.11 - Best fitness vs. generation number plot for sample run #2

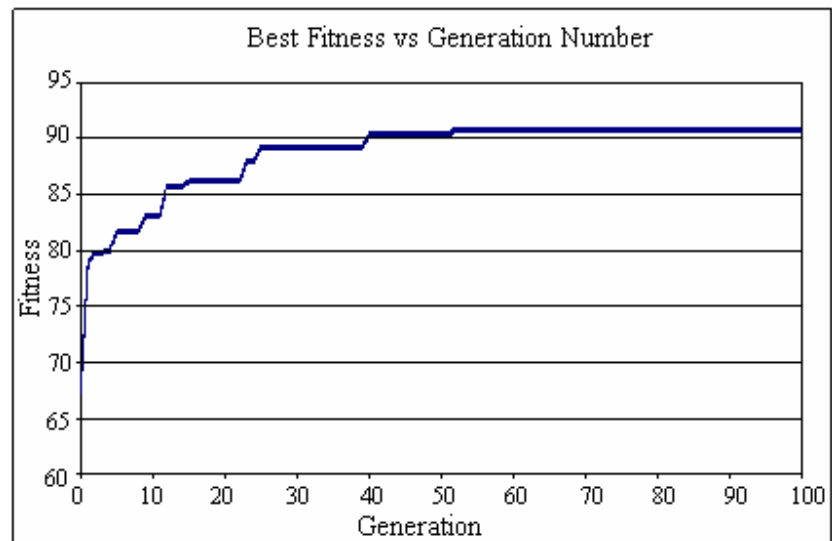Figure 7.12 - Best fitness vs. generation number plot for sample run #3

Figure 7.13 - Best fitness vs. generation number plot for sample run #4

CHAPTER 8

DISCUSSION & CONCLUSION

In this study, a computer software is developed to perform the shape optimization of the lower chassis of the wheeled excavator automatically by using Genetic Algorithm method.

The FEA of the structure is performed for a set of specified critical boundary conditions. The developed program is capable of creating finite element models of the structure defined with varying shape parameters.

The lower chassis must have minimum weight to minimize material, labour and operation costs while satisfying required fatigue strength. Mass of each model is found by means of the mass evaluation feature of the pre-processor FEM program.

In general, local maximum stress values occur at the welded regions of the structure and fatigue failure occurs in these regions. Hence, the stress data in the welded regions is considered and acquired from results file of FEA. Objective function consisting of the stress and the mass data of the structure is tried to be minimized. The optimization algorithm used by Uzer [5] is modified and embedded in the developed program. The basic parameters of the optimization process based on the genetic algorithm method are rearranged and the flowchart of the algorithm transformed to an appropriate form suitable for this study.

After embedding the optimization algorithm in the developed program, case studies are performed. One of the initial parameter sets is taken from the existing design of the lower chassis for each sample run. Approximately 15% improvement in maximum Von Mises stress is achieved without increasing the weight of the structure.

In this study, the lower chassis of HMK 200 W-2 is optimized. However, the developed program can be used for lower chassis of other types of wheeled-excavators by changing the parameters.

Fatigue failure of the weldments is the most important problem of the structure. In this study, the welding material is not simulated. The stress data is collected from the regions that are the predetermined distance away from the connection lines of the welded plates. However, fatigue life of the structure can be estimated more accurately by using fracture mechanics [17]. Implementing a sub-modelling algorithm to the developed program would be good future work. The boundary conditions of sub-model can be taken from the results file of the developed program. Therefore, fatigue life estimation can be performed more accurately for specific welded regions.

REFERENCES

[1]   SAE J1116 REV. NOV2004: Categories of Off-Road Self-Propelled Work Machines

[2]   E. A. Avallone, T. Baumaister III, Marks' Standard Handbook for Mechanical Engineers, 10th edition, McGRAW-HILL International editions, 1997.

[3]   ISO 6165:2006 : Earth-moving machinery – Basic types – Identifications and terms and definitions

[4]   Wikipedia The Free Encyclopedia
       http://en.wikipedia.org/wiki/Excavator, Last accessed date: 26.05.2008.

[5]   Uzer C., Shape Optimization of an Excavator Boom by Using Genetic Algorithm, Ms. Thesis Submitted to Middle East Technical University, Turkey, 2008.

[6]   Kyung K. Choi, Nam H. Kim, Structural Sensitivity Analysis and Optimization, Springer Science Business Media Inc., USA, 2005.

[7]   Hobbacher A., Fatigue Design of Welded Joints and Components: Recommendations of IIW Joint Working Group XIII – XV, Abington, Cambridge, 1996

[8]   Saitou K., Izui K., Nishiwaki S., Papalambros P., A Survey of Structural Optimization in Mechanical Product Development, Journal of Computing and Information Science in Engineering 5 (2005) 214-226

[9]   Xie Y., Steven G., Evolutionary Structural Optimization, Springer-Verlag London Limited, Great Britain, 1997

[10] Tanskanen P., A multiobjective and fixed elements based modification of the evolutionary structural optimization method, Comput. Methods Appl. Mech. Engrg. 196 (2006) 76-90

[11] Rastogi N., Stress Analysis and Lay-Up Optimization of an All-Composite Pick-Up Truck Chassis Structure, SAE 2004 World Congress & Exhibition, USA, March 2004, 2004-01-1519.

[12] Fasel U.M., König O., Wintermantel M., Ermanni P., Using Evolutionary Methods with a Heterogeneous Genotype Representation for Design Optimization of a Tubular Steel Trellis Motorbike-Frame. http://felyx.sourceforge.net/downloads/PAPER-Frame-Optimization.pdf, Last accessed date: 12.08.2008.

[13] Gadus J., Optimization of frameworks by means of FEM use, Research in Agricultural Engineering 49 (2003) 32-36.

[14] Lee S., Kwak B., Automatic Generation of Orthogonal Arrays for the Taguchi Method and Applications to Structural Optimal Design, Transactions of the Korean Society of Mechanical Engineers 27-12 (December 2003) 2047-2054.

[15] Lee S., Kwak B., A Versatile Structural Optimization System Based on the Taguchi Method, Korea Advanced Institute of Science and Technology (2002)

[16] Hai X., Jian S., Failure Analysis and Optimization Design of a Centrifuge Rotor, Engineering Failure Analysis 14 (2007) 101-109.

[17] Martinsson J., Fatigue Assessment of Complex Welded Steel Structures, Doctoral Thesis Submitted to Division of Lightweight Structures at Department of Aeronautical and Vehicle Engineering at the Royal Institute of Technology, Stockholm, 2004.

[18] Das R., Jones R., Design of structures for optimal static strength using ESO, Engineering Failure Analysis 12 (2005) 61-80.

[19] Conle F., Chu C., Fatigue Analysis and the Local Stress-Strain Approach in Complex Vehicular Structures, International Journal of Fatigue 19 (1997) 317-323.

[20] Sonsino C., Kueppers M., Zhang G., Fatigue Strength of Laser Beam Welded Thin Steel Structure under Multiaxial Loading, International Journal of Fatigue 28 (2006) 657-662.

[21] Yener M., Design of a Computer Interface for Automatic Finite Element Analysis of an Excavator Boom, Ms. Thesis Submitted to Middle East Technical University, Turkey, 2005.

[22] Karaoğlu C., Kuralay S., Stress Analysis of a Truck Chassis with Riveted Joints, Finite Elements in Analysis and Design 38 (2002) 1115-1130.

[23] Barton A., Integrating Manufacturing Issues into Structural Optimization, Doctoral Thesis Submitted to Aerospace, Mechanical and Mechanical Engineering at the University of Sydney, Australia, 2002.

[24] Tekkaya E., Güneri A., Shape Optimization with the Biological Growth Method: a Parameter Study, Engineering Computations 13-8 (1996) 4-18.

[25] Schneider J., Stochastic Optimization, Springer Science Business Media Inc., USA, 2006.

[26] Youssef H., Sait S., Adiche H., Evolutionary Algorithms, Simulated Annealing and Tabu Search: a Comparative Study, Engineering Applications of Artificial Intelligence 14 (2001) 167-181.

[27] Goldberg D., Genetic Algorithms in Search, Optimization and Machine Learning, Addison-Wesley Publishing Company Inc., USA, 1989.

[28] SAE J1179 REV. DEC2002: Hydraulic Excavator and Backhoe Digging Forces